Annex 6
Comparison of national emissions inventory with inverse estimates from atmospheric observations

This annex was produced and funded through the EU Horizon 2020 PARIS project (GA101081430).

Work Package Leads:
Anita Ganesan (University of Bristol, UK),
Alistair Manning (UK Met Office),
Stephan Henne (Empa, Switzerland)

1 Introduction

In this document, global concentration trends and national emissions estimates derived from atmospheric observations ("inverse estimates") are presented for most reported gases. Comparing the emissions submitted in national inventories with those calculated using atmospheric observations allows for emissions to be assessed using two fundamentally different approaches. Substantial differences can highlight areas that could warrant further investigation.

Global concentration trends for each gas are first shown using annual average concentrations from Mace Head, Ireland (Northern Hemisphere) and Kennaook/Cape Grim, Tasmania, Australia (Southern Hemisphere). Data from these stations were selected to exclude regionally-polluted air masses and therefore represents northern and southern hemispheric concentration trends. Mace Head observations were supported by the National Aeronautics and Space Administration (NASA) and the UK Department of Energy, Security and Net Zero (DESNZ), and Kennaook/Cape Grim observations by NASA and the Australian Bureau of Meteorology.

Observations of European concentrations of greenhouse gases used to derive national inverse emission estimates were collected from many different networks and providers. Methane and nitrous oxide concentrations originated from the European ICOS (Integrated Carbon Observation System) network, the UK DECC (Deriving Emissions related to Climate Change) network and other national or individual initiatives. F-gas observations were made by affiliates of the AGAGE (Advanced Global Atmospheric Gases Experiment) network. Observations from additional stations across Europe were supported by the Horizon-EU PARIS (Process Attribution of Regional Emissions) project. The observation stations used to derive emissions for each gas are shown in the corresponding sections of this document.

An atmospheric transport model provides the link between surface fluxes and concentrations measured at the observing stations. If not otherwise mentioned, inversion-based emissions estimates were derived using two atmospheric transport models combined with three inverse models, yielding a total of six inversions. This ensemble of six inversions allows us to better quantify the uncertainties associated with inverse modelling.

The two atmospheric transport models used are the Numerical Atmospheric dispersion Modelling Environment (NAME, Jones et al., 2007), and the FLEXible PARTicle dispersion model (FLEXPART, Stohl et al., 2005). Both models are backwards-running Lagrangian Particle Dispersion Models (LPDMs) that simulate the recent transport of air to each observing station. The two LPDMs have been widely used in the estimation of greenhouse gas emissions (Ganesan et al., 2015; Rigby et al., 2019; Manning et al., 2021; Henne et al., 2016).

The three inverse methods used are InTEM (Inversion Technique for Emission Modelling, Manning et al., 2021), ELRIS (Empa Lagrangian Regional Inversion System, Henne et al., 2016; Katharopoulos et al., 2023), and RHIME (Regional Hierarchical Inverse Modelling Environment, Ganesan et al., 2014). All three inverse methods estimate emissions within Europe along with boundary conditions that account for the concentration of the air entering Europe. All three systems started from the same set of a priori emissions that were either derived from the global EDGAR emission inventory (version 8, European Commission: Joint Research et al., 2023) or a uniform land-based emission, depending on the gas. A natural emission component, from the WETCHARTS product, was included in the methane prior. The same observational dataset was used by each inverse model, but data selection (i.e., filtering datasets for specific conditions) and treatment of uncertainties were chosen separately and hence differ. The three methods also differ in their statistical approaches for estimating emissions.

Emission estimates are presented for the period 2008-2024. Emissions for the full 2008-2024 period were derived with the InTEM-NAME inversion only, while emissions from 2017-2024 are presented as the mean of the six inversions (denoted the "PARIS mean"). The uncertainty shown is the minimum/maximum of the uncertainties in the ensemble.

All inversions employed a resolution of one month for CH_4 and N_2O and 1-year for the fluorinated gases. The inversion results used to compare with the inventories are a one-year calendar average for CH_4 and N_2O and the yearly value derived from a 3-year moving average for the fluorinated gases. For the 2008-2024 InTEM-NAME results, a 3-year moving average was also applied to the annualised CH_4 and N_2O results due to lack of observational coverage in the earlier years.

2 Global Concentration Trends

2.1 Methane (CH_4)

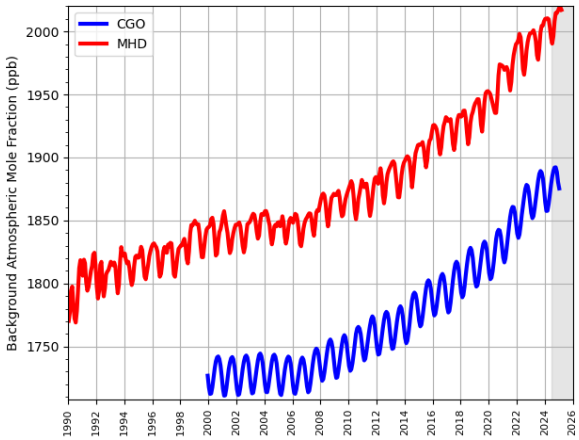

Figure 2.1.1: Background Northern Hemisphere monthly concentrations of CH_4 estimated from MHD, Ireland observations are shown in red, and background Southern Hemisphere monthly concentrations from CGO, Tasmania are shown in blue. Grey shading represents provisional data.

2.2 Nitrous Oxide (N_2O)

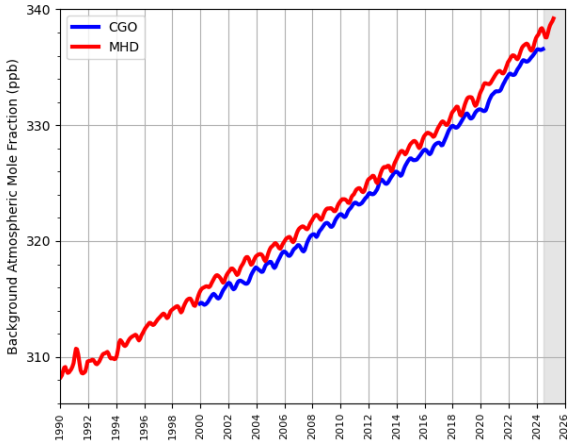

Figure 2.2.1: Background Northern Hemisphere monthly concentrations of N_2O estimated from MHD, Ireland observations are shown in red, and background Southern Hemisphere monthly concentrations from CGO, Tasmania are shown in blue. Grey shading represents provisional data.

2.3 Hydrofluorocarbons (HFCs)

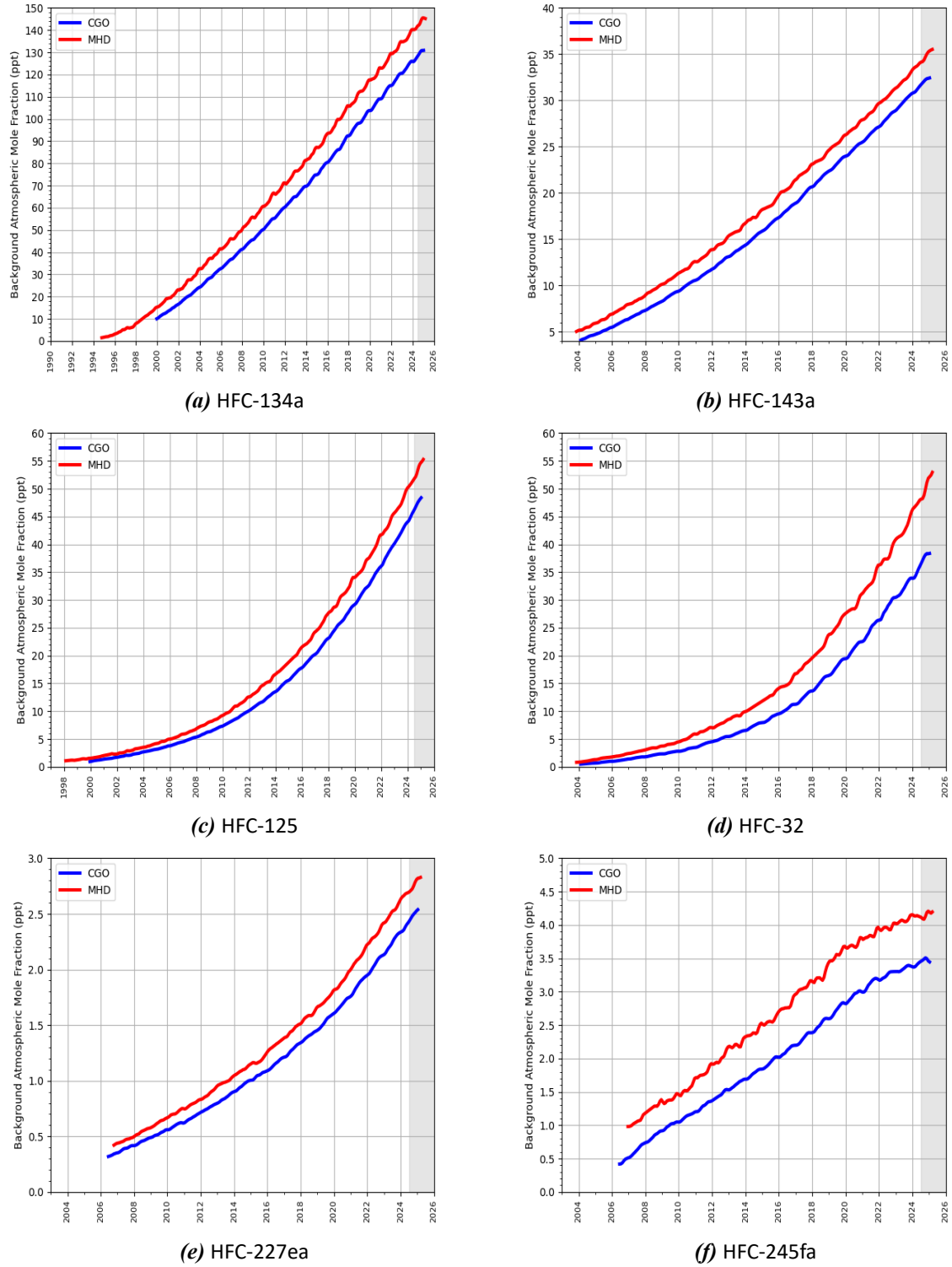

(a) HFC-134a

(b) HFC-143a

(c) HFC-125

(d) HFC-32

(e) HFC-227ea

(f) HFC-245fa

Figure 2.3.1: Background Northern Hemisphere monthly concentrations of six HFCs estimated from MHD, Ireland observations are shown in red, and background Southern Hemisphere monthly concentrations from CGO, Tasmania are shown in blue. Grey shading represents provisional data.

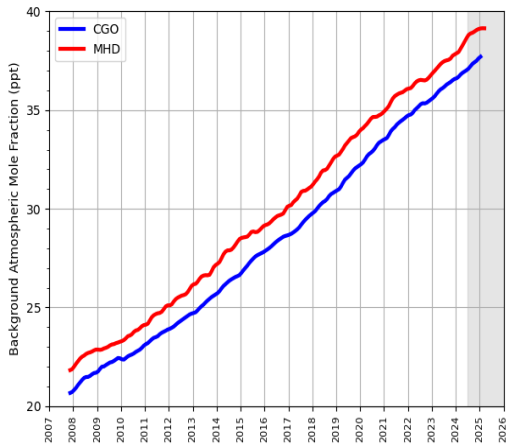

(a) HFC-23

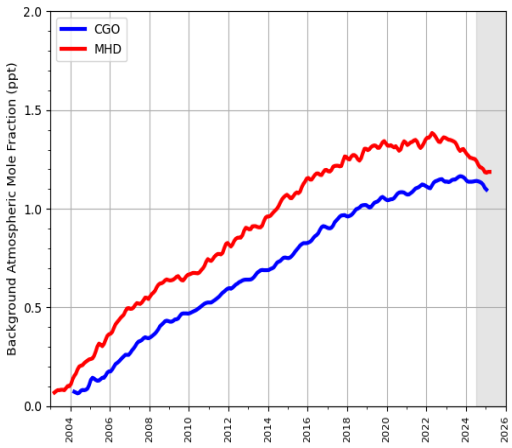

(b) HFC-365mfc

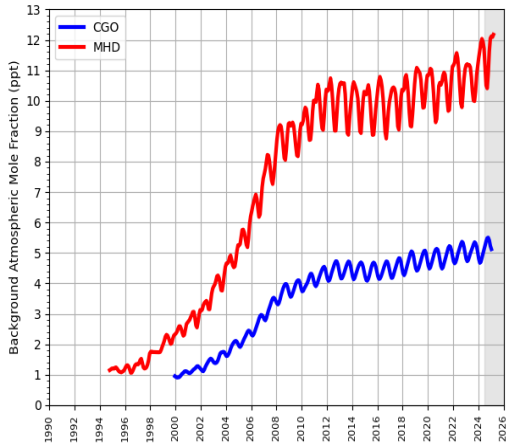

(c) HFC-152a

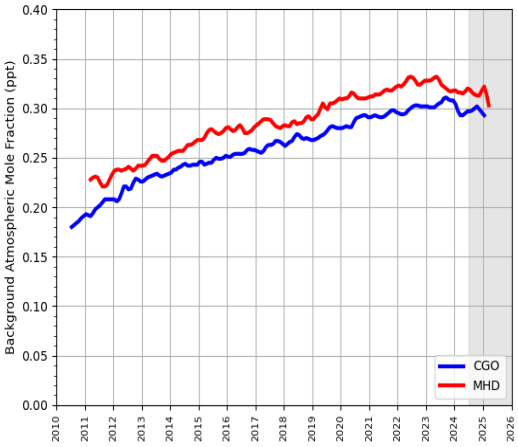

(d) HFC-43-10-mee

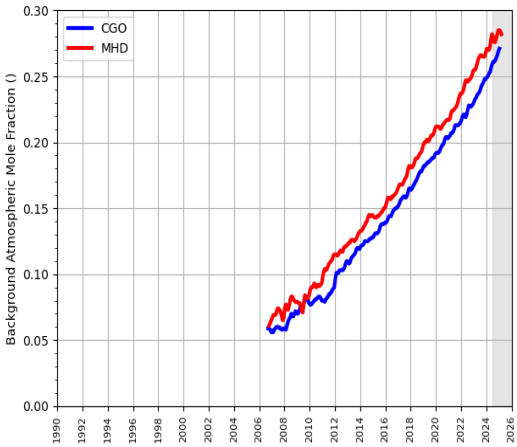

(e) HFC-236fa

Figure 2.3.2: Background Northern Hemisphere monthly concentrations of four HFCs estimated from MHD, Ireland observations are shown in red, and background Southern Hemisphere monthly concentrations from CGO, Tasmania are shown in blue. Grey shading represents provisional data.

2.4 Perfluorocarbons (PFCs)

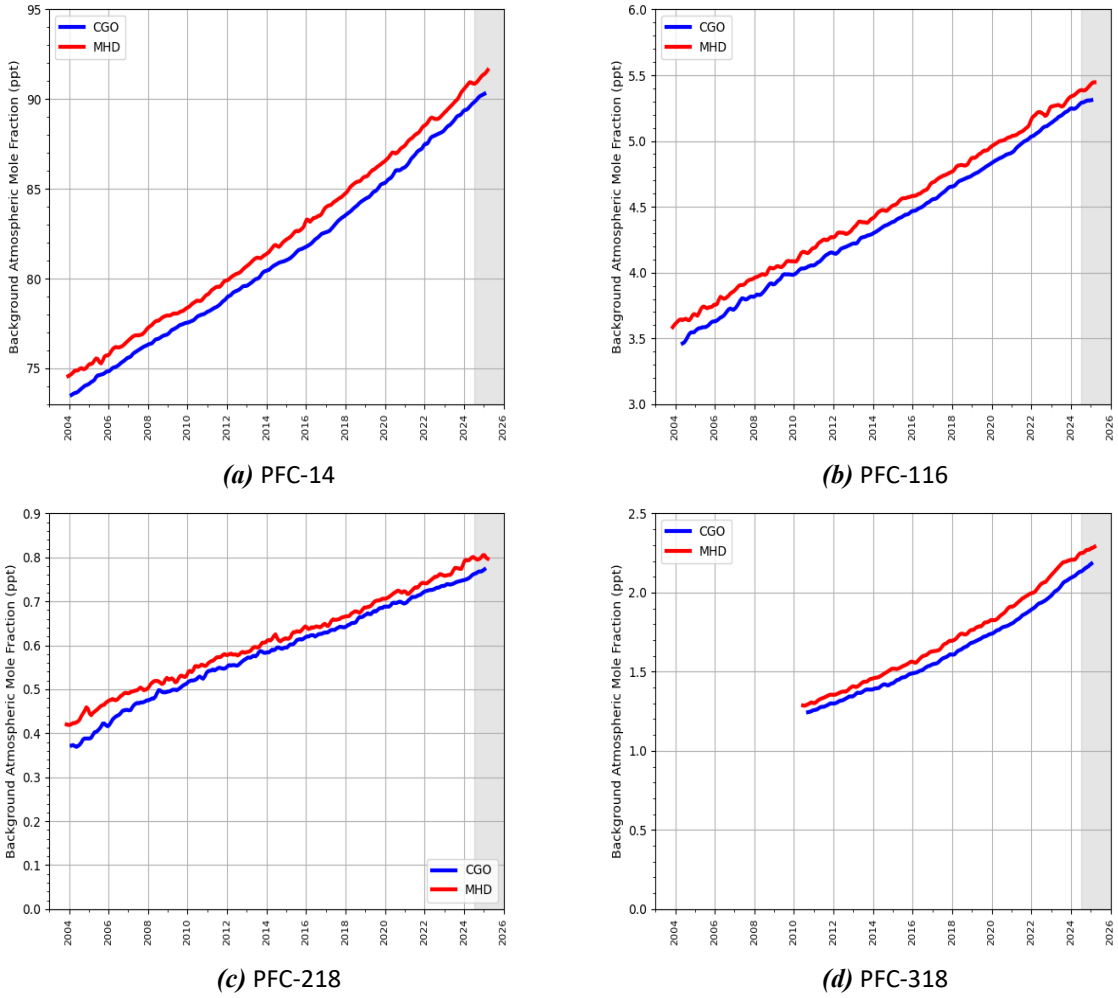

Figure 2.4.1: Background Northern Hemisphere monthly concentrations of four PFCs estimated from MHD, Ireland observations are shown in red, and background Southern Hemisphere monthly concentrations from CGO, Tasmania are shown in blue. Grey shading represents provisional data.

2.5 Sulphur Hexafluoride (SF_6) and Nitrogen Trifluoride (NF_3)

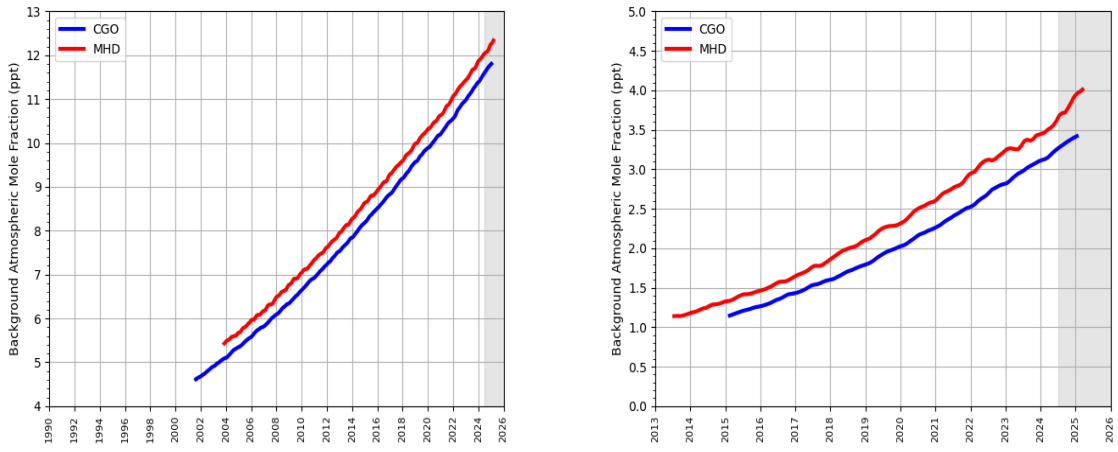

(a) SF_6 *(b)* NF_3

Figure 2.5.1: Background Northern Hemisphere monthly concentrations of SF_6 and NF_3 estimated from MHD, Ireland observations are shown in red, and background Southern Hemisphere monthly concentrations from CGO, Tasmania are shown in blue. Grey shading represents provisional data.

2.6 Carbon Dioxide (CO_2)

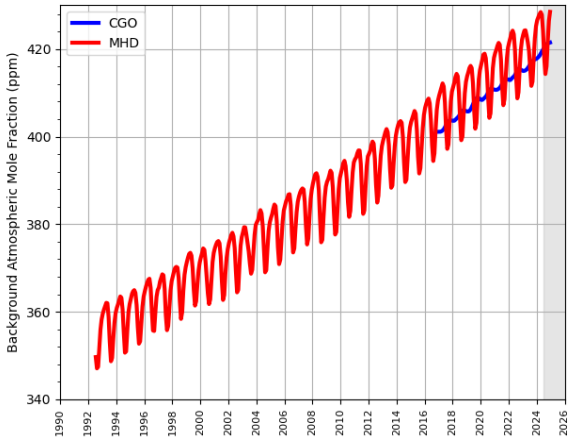

Figure 2.6.1: Background Northern Hemisphere monthly concentrations of CO_2 estimated from MHD, Ireland observations are shown in red, and background Southern Hemisphere monthly concentrations from CGO, Tasmania are shown in blue. Grey shading represents provisional data.

3 Key findings

- Methane (CH_4): Inversion results are on average ~20% lower than the inventory estimates from 2020 onwards. There does not appear to be a strong seasonal cycle in the emissions.
- Nitrous oxide (N_2O): Inversion results are on average ~12% higher than the inventory estimates from 2020 onwards. Over the last eight years the inverse results show declining emissions. A decline is seen in the inventory from 2021. In all years the inverse models estimate a pronounced seasonal cycle in emissions with the maximum in late spring or early summer. It is also noted there is year-to-year variability in the seasonal cycle.
- Hydrofluorocarbons (HFCs): The emission estimates from the inverse models for HFC-125, HFC-134a, HFC-152a and HFC-32 agree, within the uncertainties, with those reported in the inventory. The sharp drop in the inventory emissions in 2018 for HFC-143a is not seen in the inversions although the inversions have a three-year smoothing imposed. The inversion results indicate a more steady decline and are significantly lower than the inventory by 2024. The inversion results for HFC-227ea are consistently lower than the inventory.
- Perfluorocarbons (PFCs): The inverse results reveal some notable areas of emission, near Dublin for PFC-14 and near Cork for PFC-116. The inverse model estimates are very low and uncertain for PFC-218 and PFC-318. The total PFC estimate is dominated by PFC-14. PFC-14 estimates indicate a growth in emissions, although the uncertainties are large, in contrast to the inventory, which has been flat or declining since 2019.
- Sulphur hexafluoride (SF_6): The emissions estimated by the inversions are consistent within the uncertainties with those reported in the inventory.
- For all three inversion systems, the emissions derived using the transport model FLEXPART (rather than NAME) are generally lower and thus broadens the overall uncertainties.

Table 1: Emissions estimation for the main greenhouse gases of focus according to the National Inventory Document (NID) 2026 and the inversions done in the PARIS project. For the PARIS estimation, the mean of the 3 inversion models is displayed, along with a range of uncertainty estimated via the half distance between the maximum and minimum uncertainties of the different models.

			2020	2021	2022	2023	2024
CH_4	$TgCO_2\text{-eq} \cdot yr^{-1}$	NID 2026	19.8	19.8	19.8	19.5	19.1
		PARIS mean	13.4 ± 4.1	16.1 ± 3.6	16.8 ± 3.5	16.4 ± 3.5	17.1 ± 4.5
N_2O	$TgCO_2\text{-eq} \cdot yr^{-1}$	NID 2026	5.89	6.06	5.67	5.24	5.29
		PARIS mean	6.84 ± 2.06	7.30 ± 1.85	6.06 ± 2.50	5.73 ± 2.31	6.21 ± 1.48
Total HFC	$TgCO_2\text{-eq} \cdot yr^{-1}$	NID 2026	0.56	0.60	0.57	0.54	0.52
		PARIS mean	0.78 ± 0.24	0.69 ± 0.22	0.59 ± 0.19	0.59 ± 0.17	0.56 ± 0.17
Total PFC	$TgCO_2\text{-eq} \cdot yr^{-1}$	NID 2026	0.06	0.06	0.05	0.03	0.04
		PARIS mean	0.07 ± 0.05	0.08 ± 0.06	0.10 ± 0.09	0.11 ± 0.09	0.12 ± 0.10
SF_6	$GgCO_2\text{-eq} \cdot yr^{-1}$	NID 2026	17	25	29	31	23
		PARIS mean	53 ± 41	37 ± 33	21 ± 36	20 ± 31	26 ± 37
NF_3	$GgCO_2\text{-eq} \cdot yr^{-1}$	NID 2026	10	9	9	8	17
		PARIS mean	6 ± 10	8 ± 18	8 ± 20	11 ± 27	11 ± 25

4 Methane (CH_4)

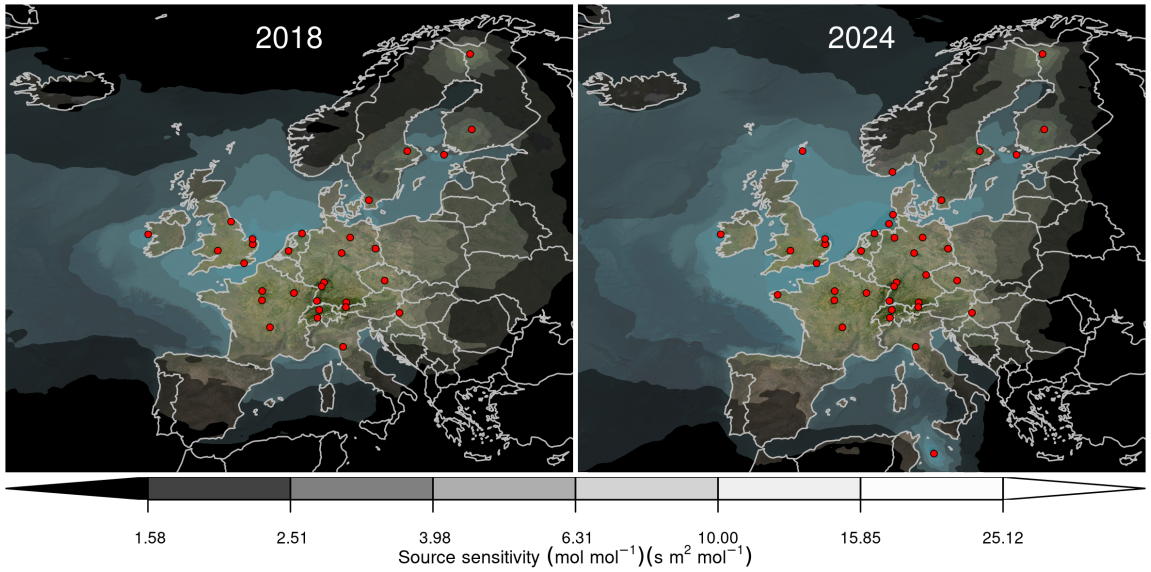

Figure 4.0.1: Average monthly total source sensitivity of CH_4 observing sites as calculated by the FLEXPART transport model for the year 2018 (left) and 2024 (right) and used in the inversions. Observing stations active in each year are marked with red dots. Areas with visible land surface represent regions for which emissions can be observed well from the network. Shaded or dark areas represent regions for which limited emission information can be obtained from the network.

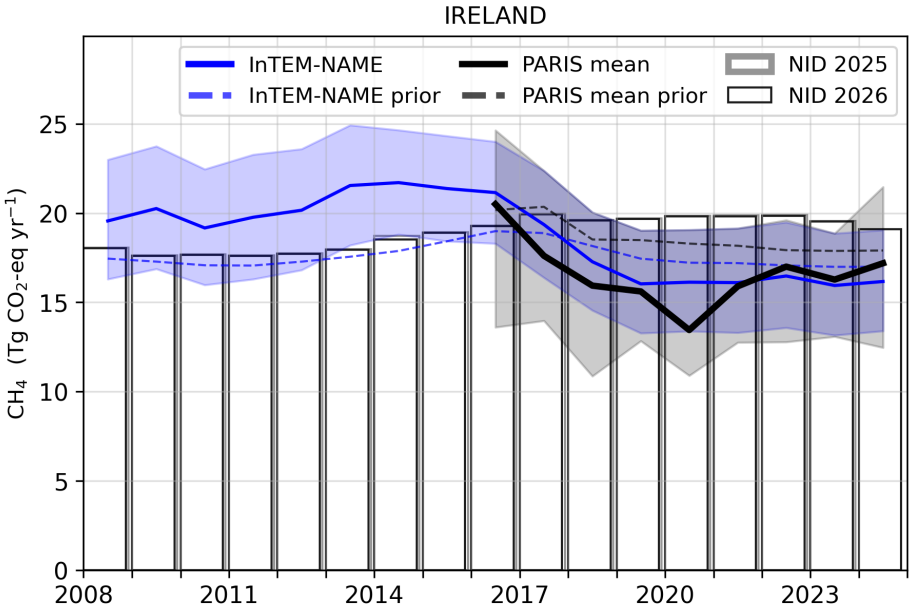

Figure 4.0.2: Verification of the Irish emissions inventory estimates for CH_4. Modelled annual emissions are given as the mean from all models (black line) and the individual result from InTEM-NAME (blue line). The shaded blue area is the 68 % confidence interval (CI) of InTEM-NAME and the shaded grey area encompasses the 68 % CI from all models. National inventory annual totals from 2025 and 2026 are given as grey and black bars, respectively.

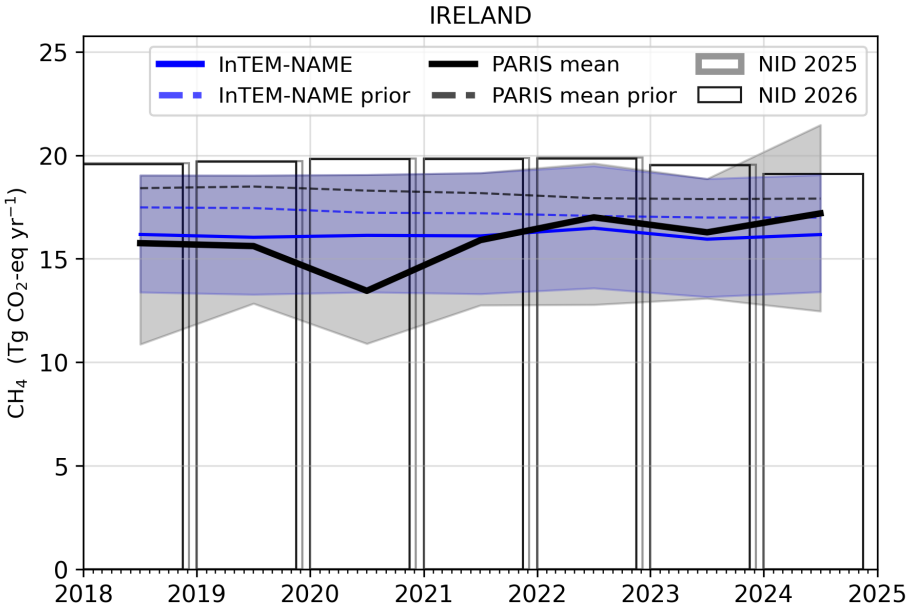

Figure 4.0.3: Verification of the Irish emissions inventory estimates for CH_4 (zoom in to 2018-2024). Modelled annual emissions are given as the mean from all models (black line) and the individual result from InTEM-NAME (blue line). The shaded blue area is the 68 % confidence interval (CI) of InTEM-NAME and the shaded grey area encompasses the 68 % CI from all models. National inventory annual totals from 2025 and 2026 are given as grey and black bars, respectively.

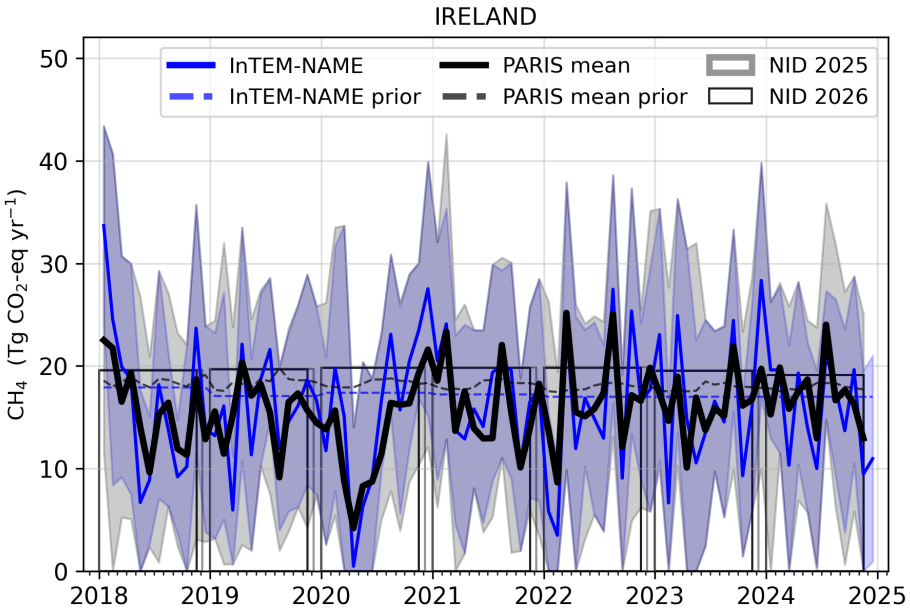

Figure 4.0.4: Verification of the Irish emissions inventory estimates for CH_4 (zoom in to 2018-2024). Modelled monthly emissions are given as the mean from all models (black line) and the individual result from InTEM-NAME (blue line). The shaded blue area is the 68 % confidence interval (CI) of InTEM-NAME and the shaded grey area encompasses the 68 % CI from all models. National inventory annual totals from 2025 and 2026 are given as grey and black bars, respectively.

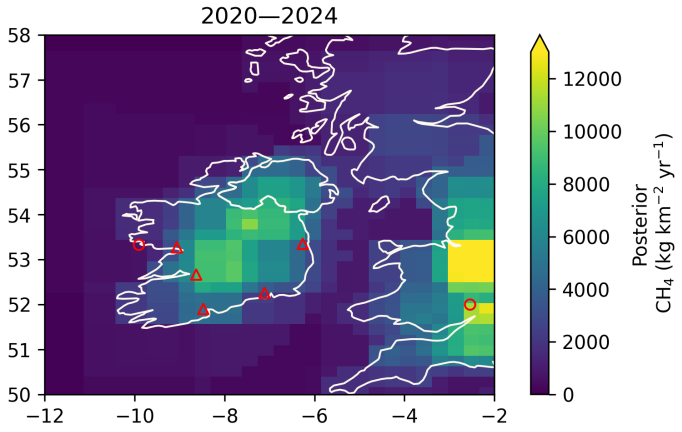

Figure 4.0.5: Spatial distribution of the Irish average modelled emissions of CH_4 during the period of 2020-2024 (mean from all models). Observing stations are marked with red circles and highly-populated cities are marked with red triangles.

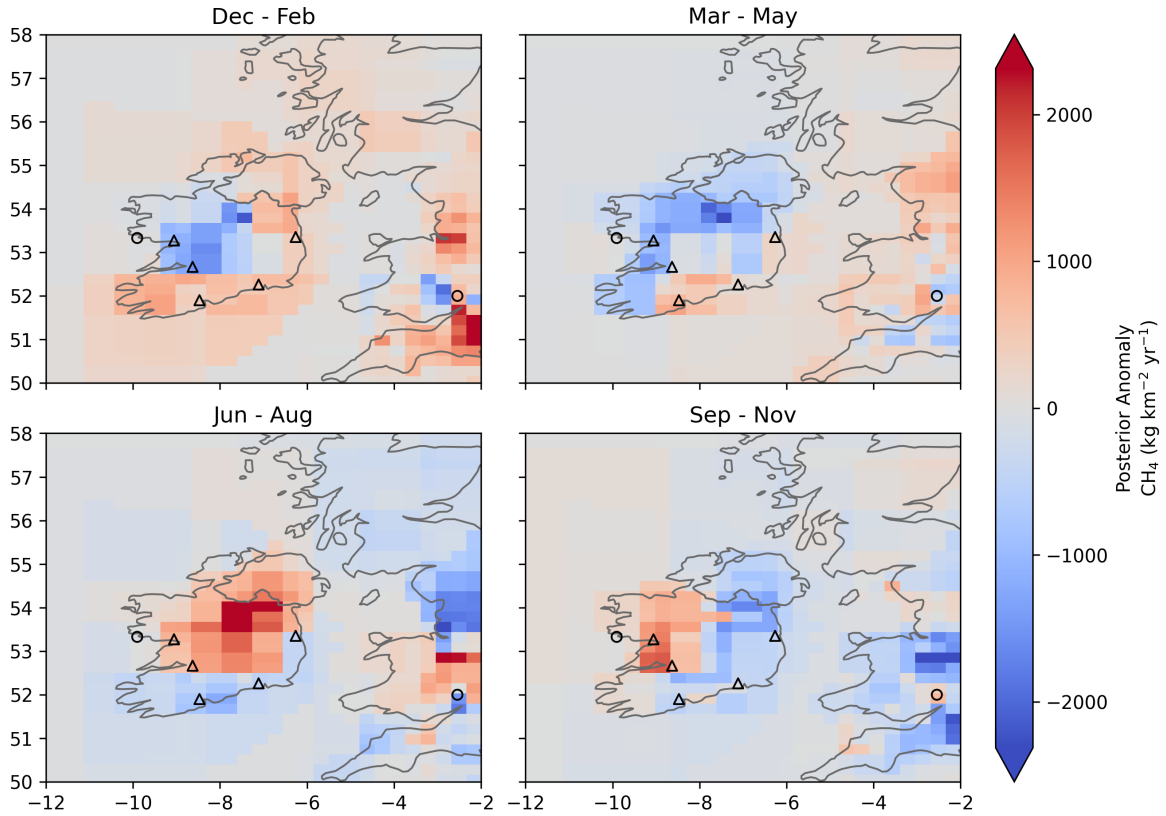

Figure 4.0.6: Spatial distribution of the seasonal deviation from the mean. The deviation is defined as the modelled Irish seasonally averaged CH_4 emissions over 2020-2024 minus the average over the whole period. The mean across all models is shown. Observing stations are marked with black circles and highly-populated cities are marked with black triangles.

5 Nitrous Oxide (N_2O)

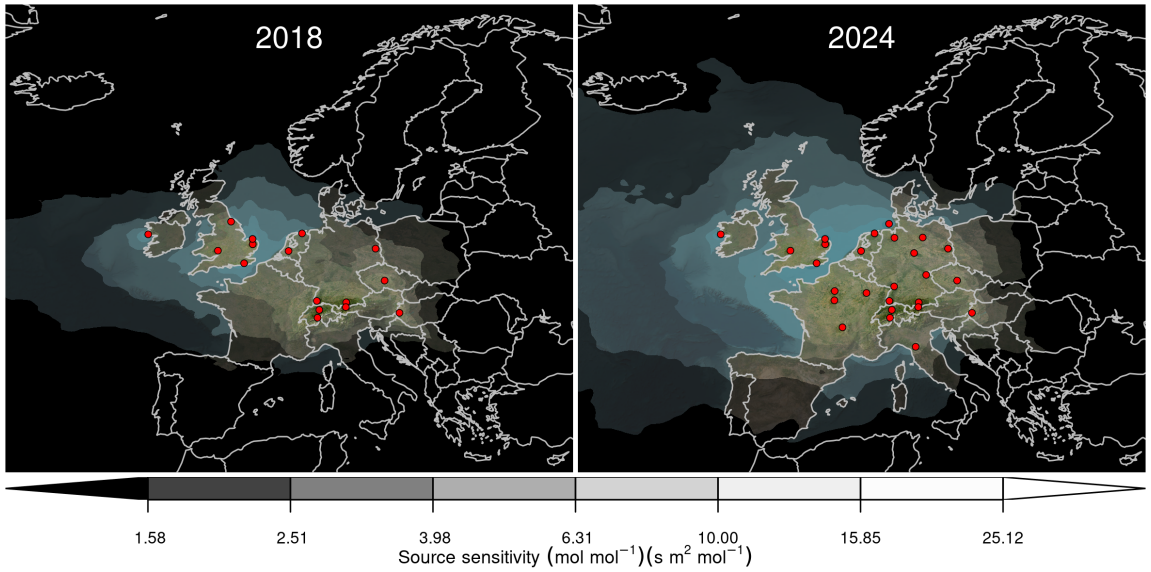

Figure 5.0.1: Average monthly total source sensitivity of N_2O observing sites as calculated by the FLEXPART transport model for the year 2018 (left) and 2024 (right) and used in the inversions. Observing stations active in each year are marked with red dots. Areas with visible land surface represent regions for which emissions can be observed well from the network. Shaded or dark areas represent regions for which limited emission information can be obtained from the network.

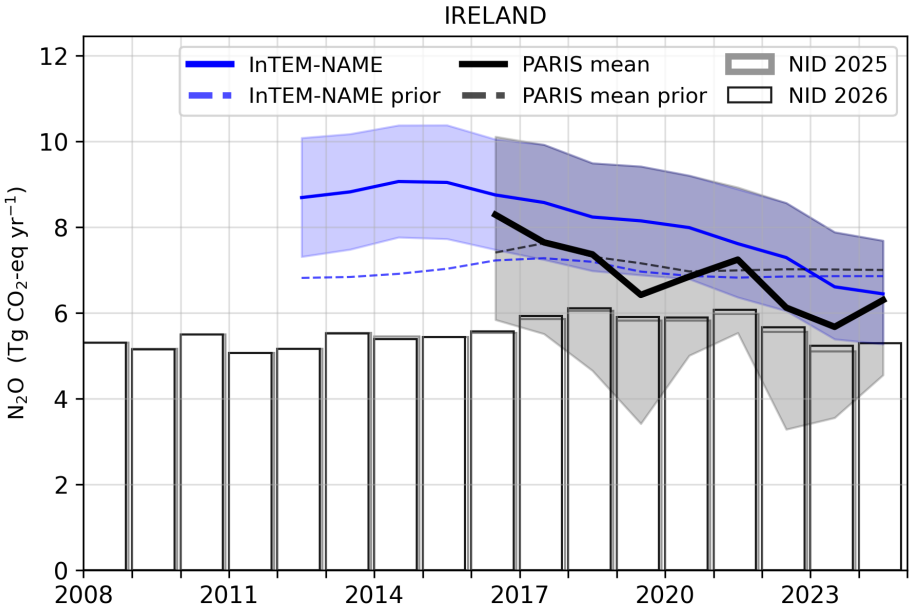

Figure 5.0.2: Verification of the Irish emissions inventory estimates for N_2O. Modelled annual emissions are given as the mean from all models (black line) and the individual result from InTEM-NAME (blue line). The shaded blue area is the 68 % confidence interval (CI) of InTEM-NAME and the shaded grey area encompasses the 68 % CI from all models. National inventory annual totals from 2025 and 2026 are given as grey and black bars, respectively.

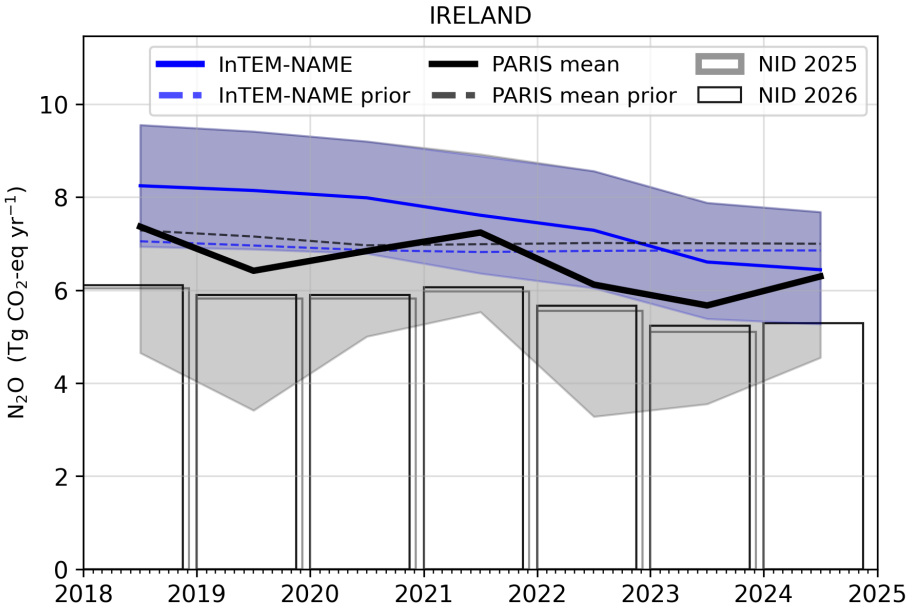

Figure 5.0.3: Verification of the Irish emissions inventory estimates for N_2O (zoom in to 2018-2024). Modelled annual emissions are given as the mean from all models (black line) and the individual result from InTEM-NAME (blue line). The shaded blue area is the 68 % confidence interval (CI) of InTEM-NAME and the shaded grey area encompasses the 68 % CI from all models. National inventory annual totals from 2025 and 2026 are given as grey and black bars, respectively.

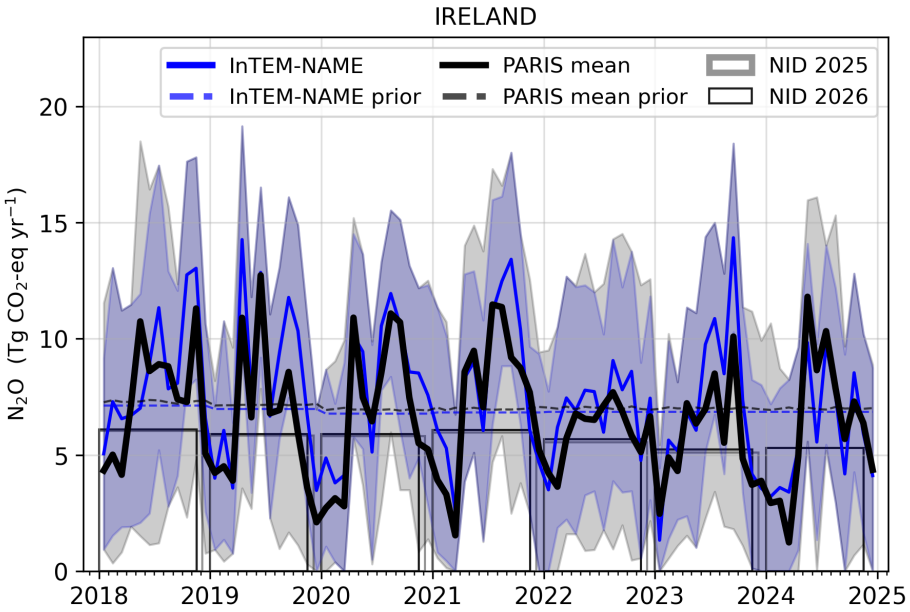

Figure 5.0.4: Verification of the Irish emissions inventory estimates for N_2O (zoom in to 2018-2024). Modelled monthly emissions are given as the mean from all models (black line) and the individual result from InTEM-NAME (blue line). The shaded blue area is the 68 % confidence interval (CI) of InTEM-NAME and the shaded grey area encompasses the 68 % CI from all models. National inventory annual totals from 2025 and 2026 are given as grey and black bars, respectively.

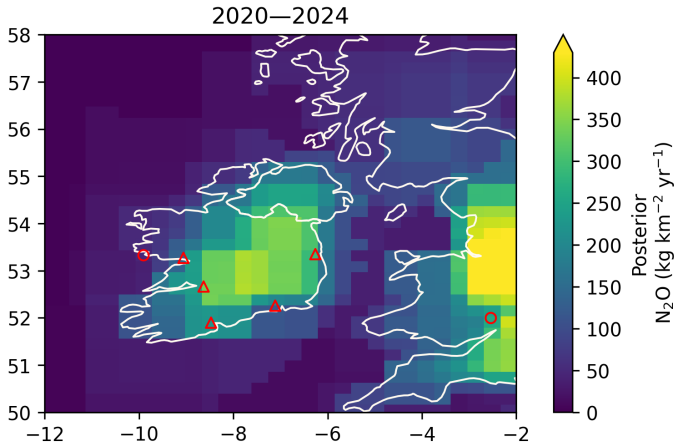

Figure 5.0.5: Spatial distribution of the Irish average modelled emissions of N_2O during the period of 2020-2024 (mean from all models). Observing stations are marked with red circles and highly-populated cities are marked with red triangles.

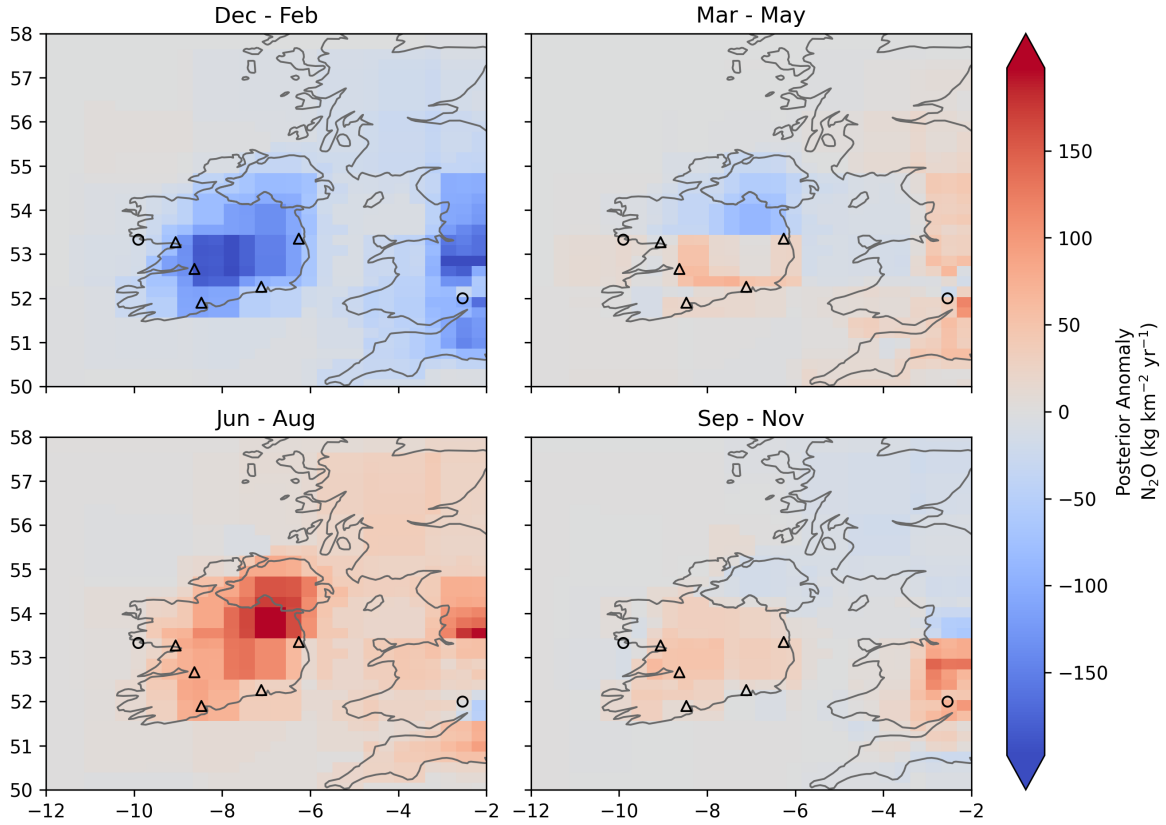

Figure 5.0.6: Spatial distribution of the seasonal deviation from the mean. The deviation is defined as the modelled Irish seasonally averaged N_2O emissions over 2020-2024 minus the average over the whole period. The mean across all models is shown. Observing stations are marked with black circles and highly-populated cities are marked with black triangles.

6 Hydrofluorocarbons (HFCs)

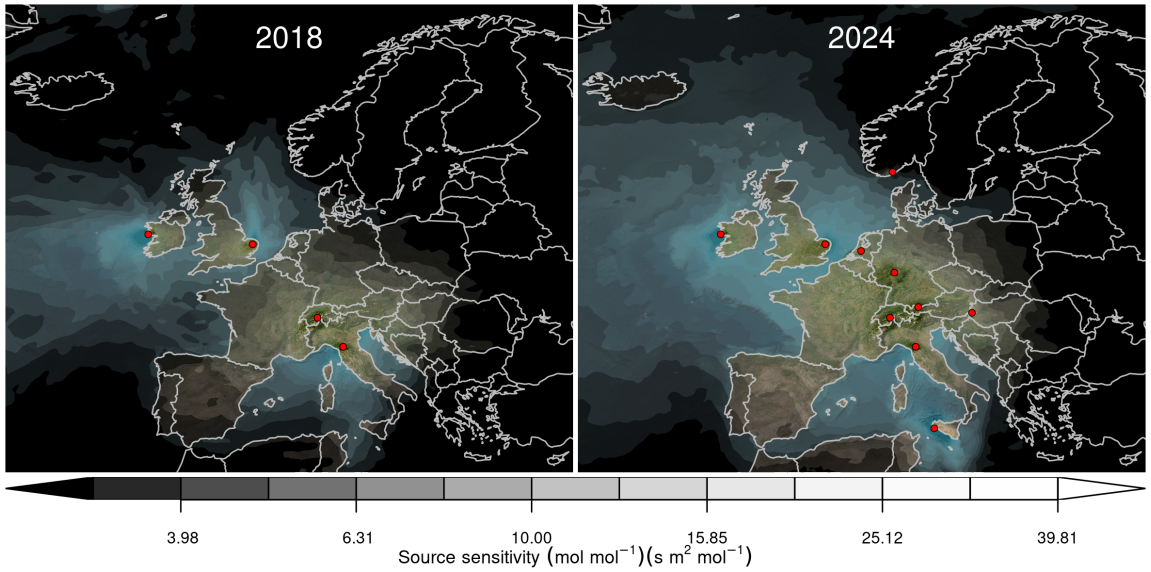

Figure 6.0.1: Total source sensitivity of HFCs/PFCs observing sites as calculated by the FLEXPART transport model for the year 2018 (left) and 2024 (right) and used in the inversions. Observing stations active in each year are marked with red dots. Areas with visible land surface represent regions for which emissions can be observed well from the network. Shaded or dark areas represent regions for which limited emission information can be obtained from the network.

6.1 HFC-125

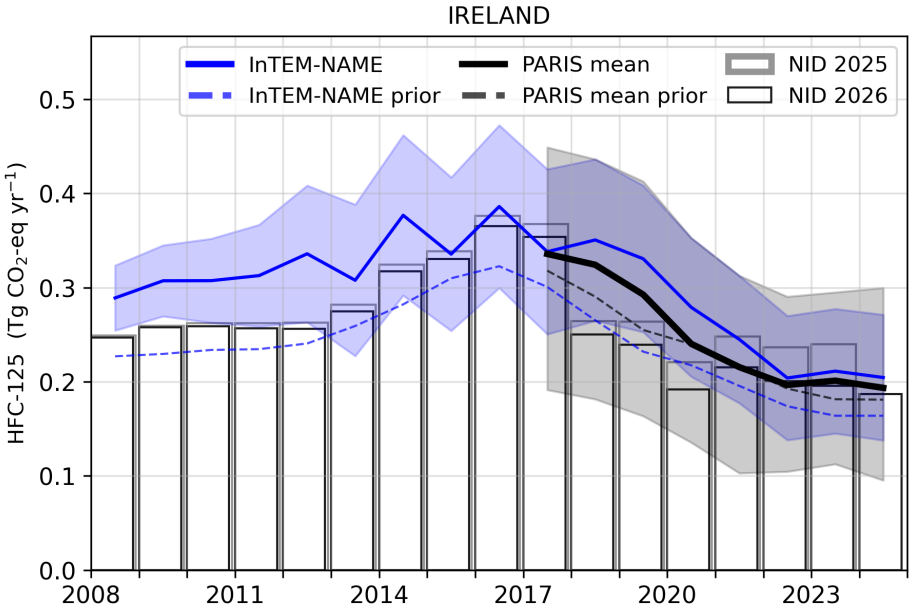

Figure 6.1.1: Verification of the Irish emissions inventory estimates for HFC-125. Modelled annual emissions are given as the mean from all models (black line) and the individual result from InTEM-NAME (blue line). The shaded blue area is the 68 % confidence interval (CI) of InTEM-NAME and the shaded grey area encompasses the 68 % CI from all models. National inventory annual totals from 2025 and 2026 are given as grey and black bars, respectively.

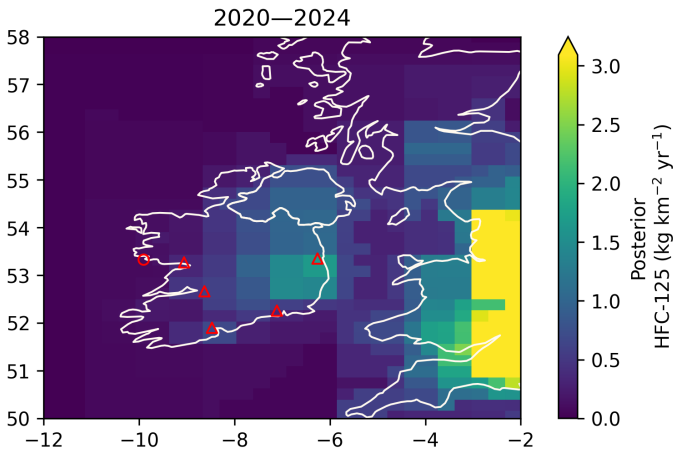

Figure 6.1.2: Spatial distribution of the Irish average modelled emissions of HFC-125 during the period of 2020-2024 (mean from all models). Observing stations are marked with red circles and highly-populated cities are marked with red triangles.

6.2 HFC-134a

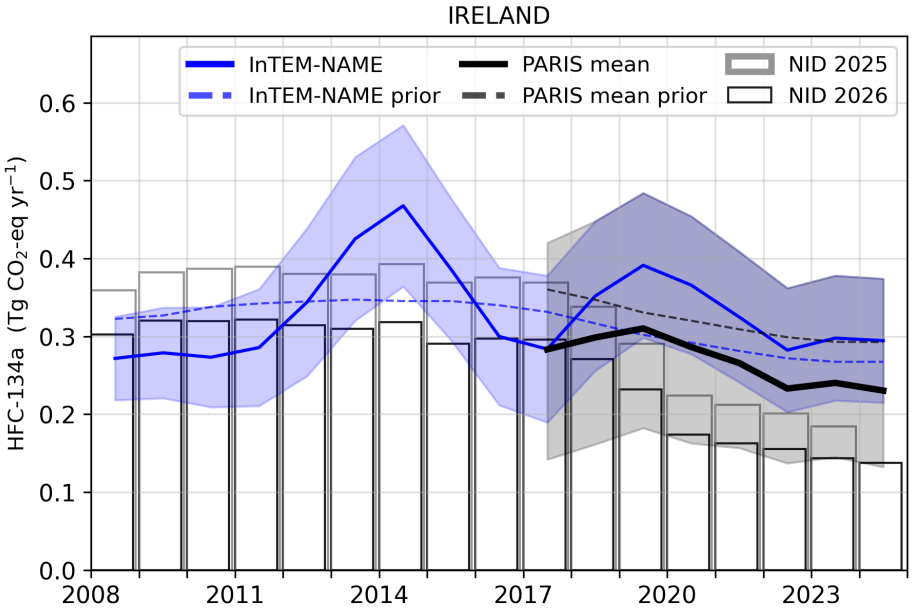

Figure 6.2.1: Verification of the Irish emissions inventory estimates for HFC-134a. Modelled annual emissions are given as the mean from all models (black line) and the individual result from InTEM-NAME (blue line). The shaded blue area is the 68 % confidence interval (CI) of InTEM-NAME and the shaded grey area encompasses the 68 % CI from all models. National inventory annual totals from 2025 and 2026 are given as grey and black bars, respectively.

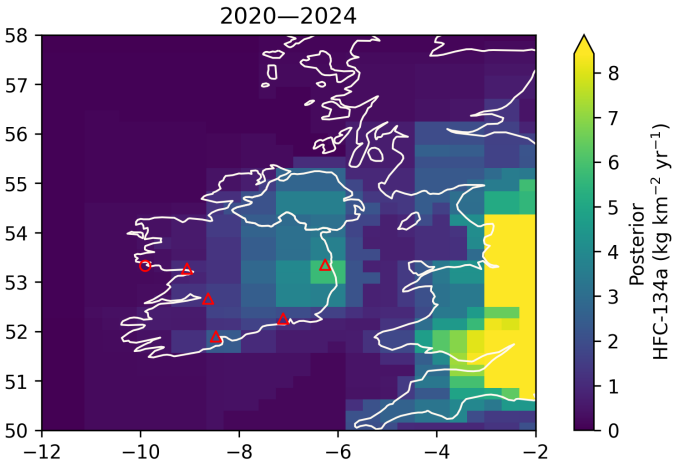

Figure 6.2.2: Spatial distribution of the Irish average modelled emissions of HFC-134a during the period of 2020-2024 (mean from all models). Observing stations are marked with red circles and highly-populated cities are marked with red triangles.

6.3 HFC-143a

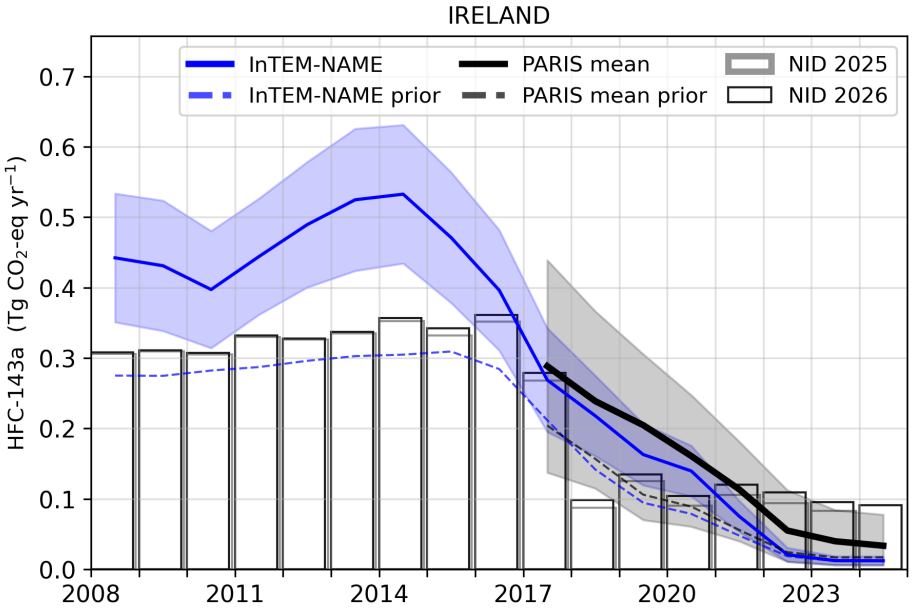

Figure 6.3.1: Verification of the Irish emissions inventory estimates for HFC-143a. Modelled annual emissions are given as the mean from all models (black line) and the individual result from InTEM-NAME (blue line). The shaded blue area is the 68 % confidence interval (CI) of InTEM-NAME and the shaded grey area encompasses the 68 % CI from all models. National inventory annual totals from 2025 and 2026 are given as grey and black bars, respectively.

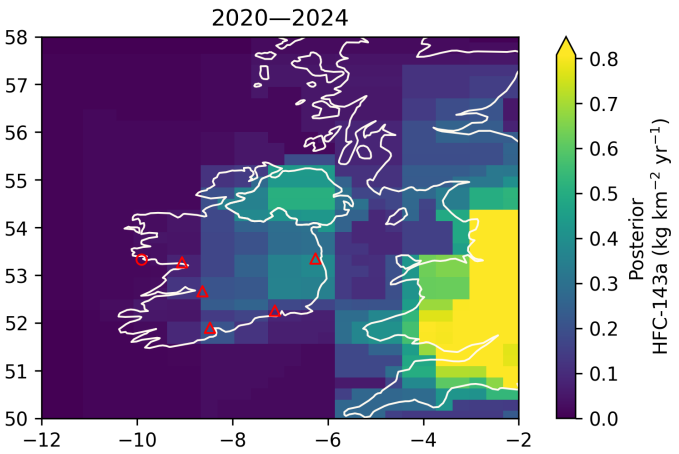

Figure 6.3.2: Spatial distribution of the Irish average modelled emissions of HFC-143a during the period of 2020-2024 (mean from all models). Observing stations are marked with red circles and highly-populated cities are marked with red triangles.

6.4 HFC-152a

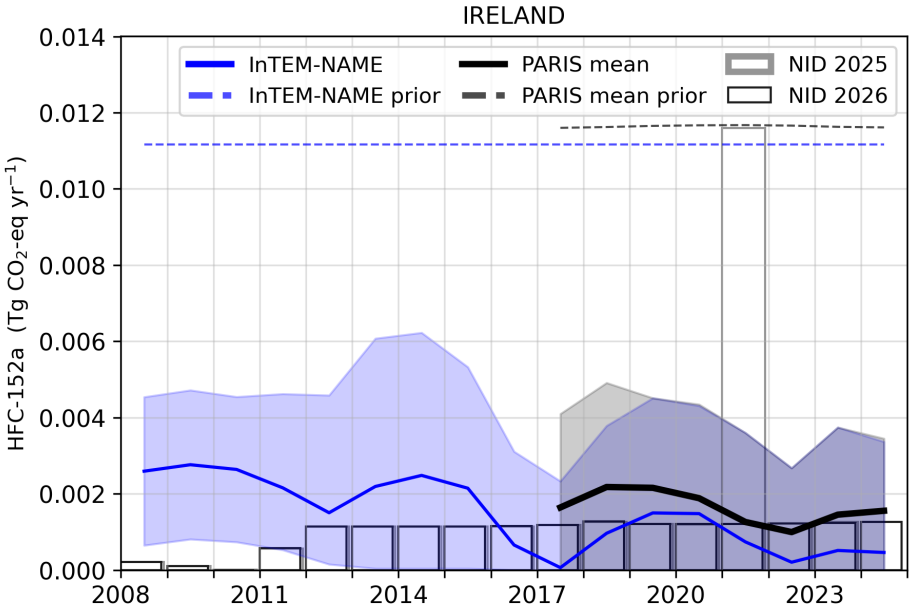

Figure 6.4.1: Verification of the Irish emissions inventory estimates for HFC-152a. Modelled annual emissions are given as the mean from all models (black line) and the individual result from InTEM-NAME (blue line). The shaded blue area is the 68 % confidence interval (CI) of InTEM-NAME and the shaded grey area encompasses the 68 % CI from all models. National inventory annual totals from 2025 and 2026 are given as grey and black bars, respectively.

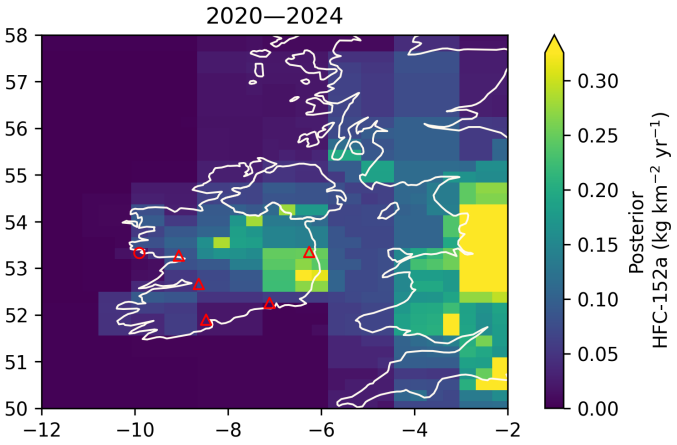

Figure 6.4.2: Spatial distribution of the Irish average modelled emissions of HFC-152a during the period of 2020-2024 (mean from all models). Observing stations are marked with red circles and highly-populated cities are marked with red triangles.

6.5 HFC-227ea

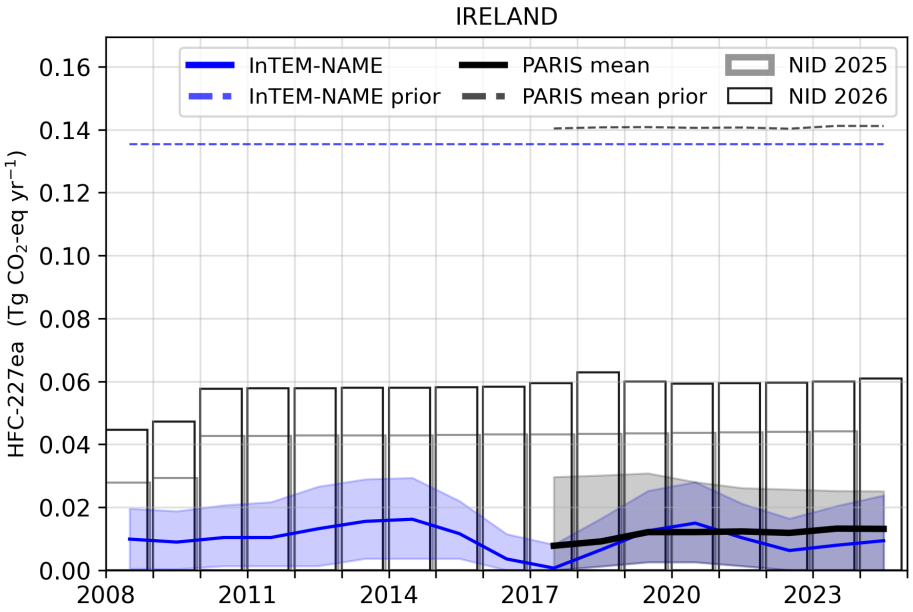

Figure 6.5.1: Verification of the Irish emissions inventory estimates for HFC-227ea. Modelled annual emissions are given as the mean from all models (black line) and the individual result from InTEM-NAME (blue line). The shaded blue area is the 68 % confidence interval (CI) of InTEM-NAME and the shaded grey area encompasses the 68 % CI from all models. National inventory annual totals from 2025 and 2026 are given as grey and black bars, respectively.

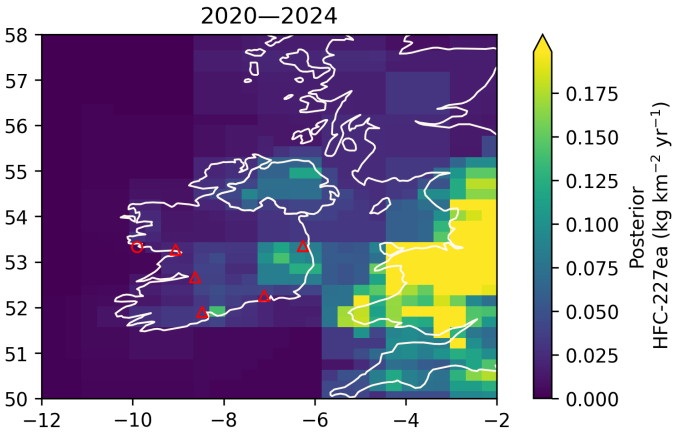

Figure 6.5.2: Spatial distribution of the Irish average modelled emissions of HFC-227ea during the period of 2020-2024 (mean from all models). Observing stations are marked with red circles and highly-populated cities are marked with red triangles.

6.6 HFC-32

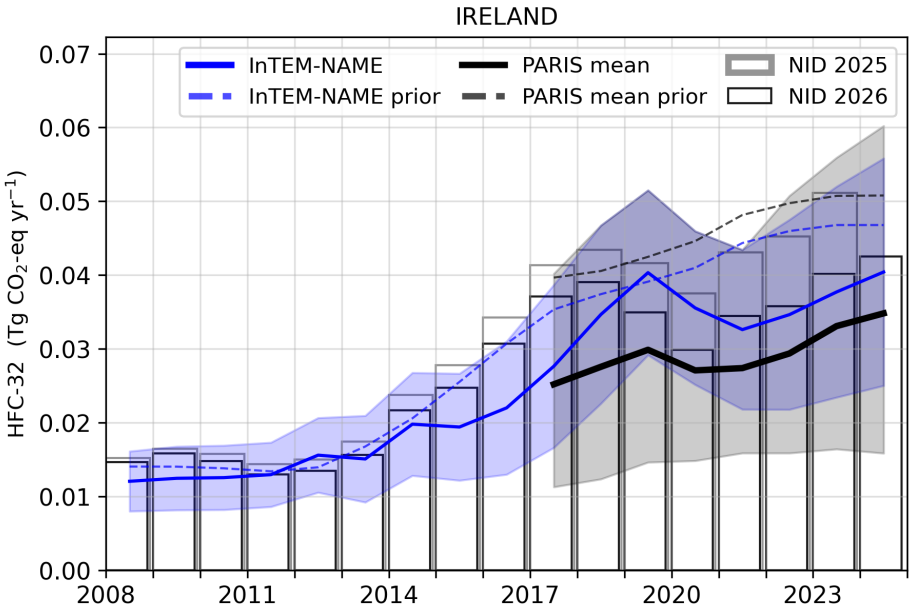

Figure 6.6.1: Verification of the Irish emissions inventory estimates for HFC-32. Modelled annual emissions are given as the mean from all models (black line) and the individual result from InTEM-NAME (blue line). The shaded blue area is the 68 % confidence interval (CI) of InTEM-NAME and the shaded grey area encompasses the 68 % CI from all models. National inventory annual totals from 2025 and 2026 are given as grey and black bars, respectively.

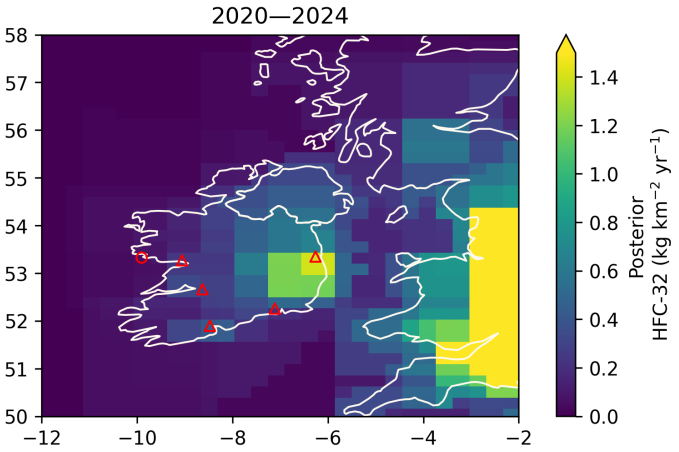

Figure 6.6.2: Spatial distribution of the Irish average modelled emissions of HFC-32 during the period of 2020-2024 (mean from all models). Observing stations are marked with red circles and highly-populated cities are marked with red triangles.

6.7 Total HFCs

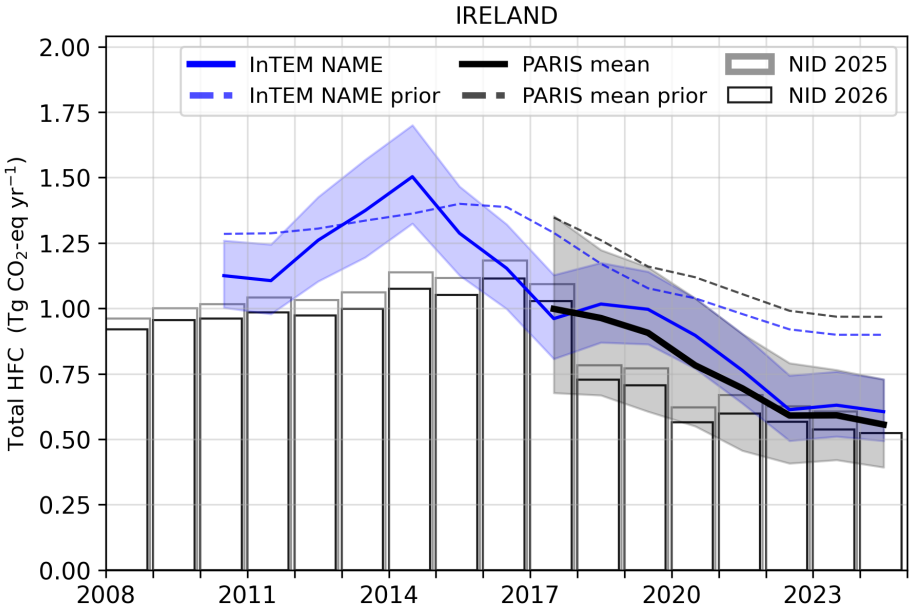

Figure 6.7.1: Verification of the Irish emissions inventory estimates for total HFCs. Modelled annual emissions are given as the mean from all models (black line) and the individual result from InTEM-NAME (blue line). The shaded blue area is the 68 % confidence interval (CI) of InTEM-NAME and the shaded grey area encompasses the 68 % CI from all models. National inventory annual totals from 2025 and 2026 are given as grey and black bars, respectively.

Table 2: Emissions estimation for HFCs according to the National Inventory Document (NID) 2026 and the inversions done in the PARIS project. For the PARIS estimation, the mean of the 3 inversion models is displayed, along with a range of uncertainty estimated via the half distance between the maximum and minimum uncertainties of the different models.

			2020	2021	2022	2023	2024
HFC-134a	$TgCO_2\text{-eq} \cdot yr^{-1}$	NID 2026	0.17	0.16	0.16	0.14	0.14
		PARIS mean	0.29 ± 0.15	0.27 ± 0.13	0.23 ± 0.11	0.24 ± 0.12	0.23 ± 0.12
HFC-125	$TgCO_2\text{-eq} \cdot yr^{-1}$	NID 2026	0.19	0.22	0.20	0.20	0.19
		PARIS mean	0.24 ± 0.11	0.22 ± 0.10	0.20 ± 0.09	0.20 ± 0.09	0.19 ± 0.10
HFC-143a	$TgCO_2\text{-eq} \cdot yr^{-1}$	NID 2026	0.10	0.12	0.11	0.10	0.09
		PARIS mean	0.16 ± 0.09	0.11 ± 0.07	0.05 ± 0.05	0.04 ± 0.04	0.03 ± 0.04
HFC-23	$GgCO_2\text{-eq} \cdot yr^{-1}$	NID 2026	4	5	4	2	3
		PARIS mean	35 ± 49	43 ± 67	51 ± 67	51 ± 67	39 ± 58
HFC-32	$GgCO_2\text{-eq} \cdot yr^{-1}$	NID 2026	30	34	36	40	42
		PARIS mean	27 ± 16	27 ± 14	29 ± 17	33 ± 20	35 ± 22
HFC-227ea	$GgCO_2\text{-eq} \cdot yr^{-1}$	NID 2026	59	59	60	60	61
		PARIS mean	12 ± 13	12 ± 12	12 ± 13	13 ± 13	13 ± 13
HFC-365mfc	$GgCO_2\text{-eq} \cdot yr^{-1}$	NID 2026	0.0	0.0	0.0	0.0	0.0
		PARIS mean	8.6 ± 7.0	8.0 ± 6.5	5.7 ± 4.9	4.5 ± 4.5	3.5 ± 3.6
HFC-245fa	$GgCO_2\text{-eq} \cdot yr^{-1}$	NID 2026	0.0	0.0	0.0	0.0	0.0
		PARIS mean	5.8 ± 8.4	4.2 ± 6.4	3.1 ± 5.5	2.5 ± 4.6	2.6 ± 4.7
HFC-236fa	$GgCO_2\text{-eq} \cdot yr^{-1}$	NID 2026	0.0	0.0	0.0	0.0	0.0
		PARIS mean	3.2 ± 5.6	2.9 ± 4.6	2.5 ± 3.6	3.2 ± 4.6	3.3 ± 4.6
HFC-152a	$GgCO_2\text{-eq} \cdot yr^{-1}$	NID 2026	1.2	1.2	1.2	1.2	1.3
		PARIS mean	1.9 ± 2.2	1.3 ± 1.8	1.0 ± 1.3	1.5 ± 1.9	1.6 ± 1.7
HFC-4310mee	$GgCO_2\text{-eq} \cdot yr^{-1}$	NID 2026	0.0	0.0	0.0	0.0	0.0
		PARIS mean	1.6 ± 3.8	1.5 ± 3.5	1.2 ± 2.5	0.9 ± 1.9	0.8 ± 1.7

7 Perfluorocarbons (PFCs)

7.1 PFC-14

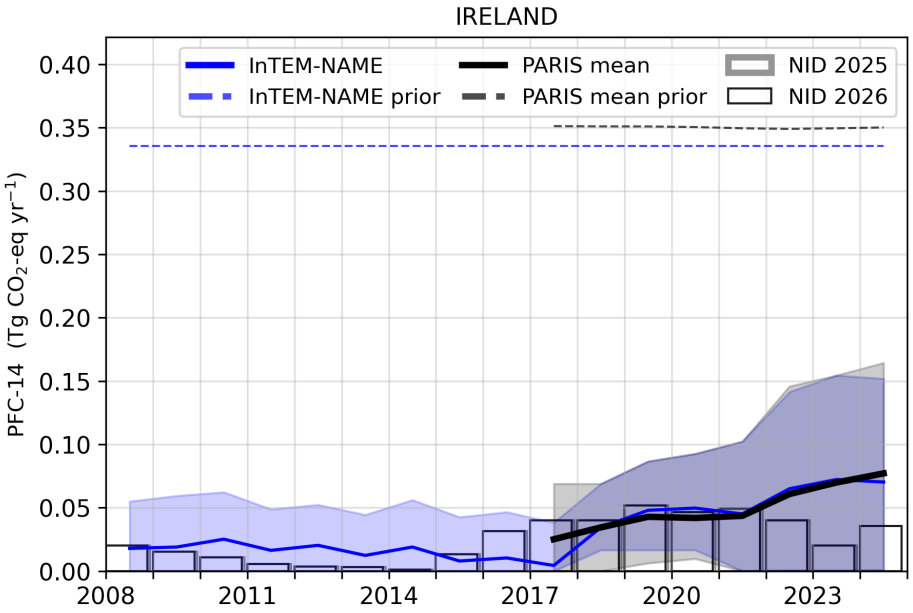

Figure 7.1.1: Verification of the Irish emissions inventory estimates for PFC-14. Modelled annual emissions are given as the mean from all models (black line) and the individual result from InTEM-NAME (blue line). The shaded blue area is the 68 % confidence interval (CI) of InTEM-NAME and the shaded grey area encompasses the 68 % CI from all models. National inventory annual totals from 2025 and 2026 are given as grey and black bars, respectively.

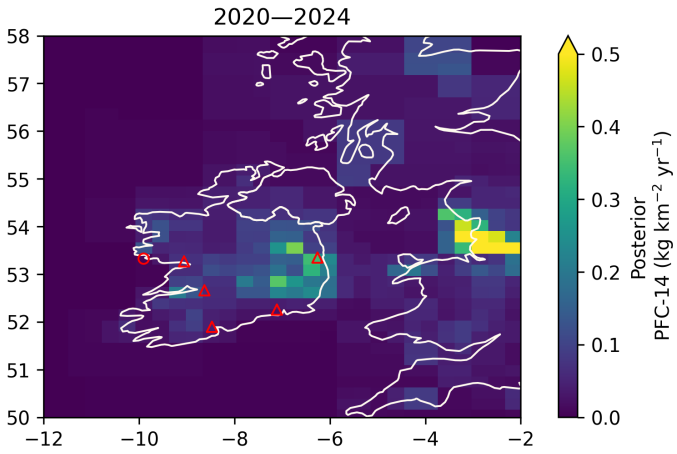

Figure 7.1.2: Spatial distribution of the Irish average modelled emissions of PFC-14 during the period of 2020-2024 (mean from all models). Observing stations are marked with red circles and highly-populated cities are marked with red triangles.

7.2 PFC-116

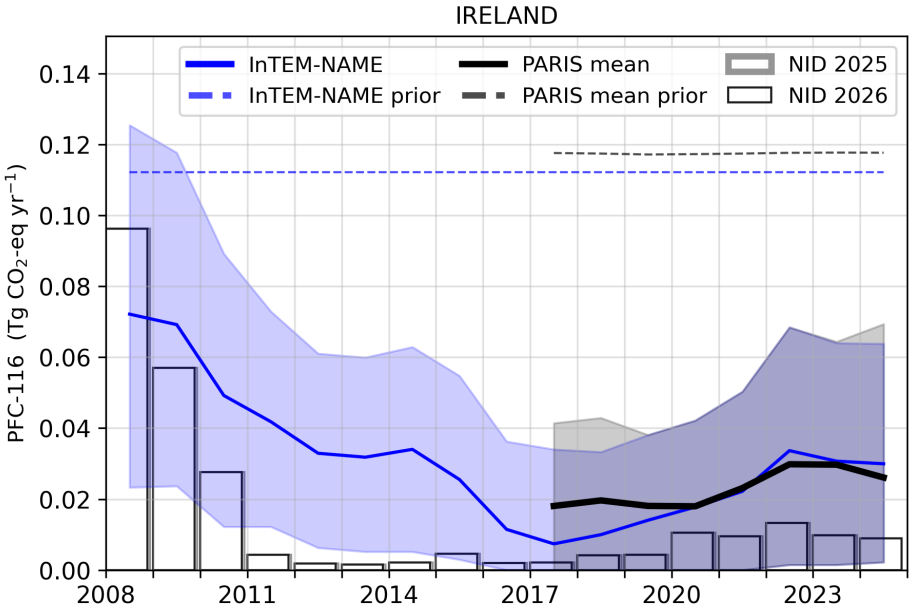

Figure 7.2.1: Verification of the Irish emissions inventory estimates for PFC-116. Modelled annual emissions are given as the mean from all models (black line) and the individual result from InTEM-NAME (blue line). The shaded blue area is the 68 % confidence interval (CI) of InTEM-NAME and the shaded grey area encompasses the 68 % CI from all models. National inventory annual totals from 2025 and 2026 are given as grey and black bars, respectively.

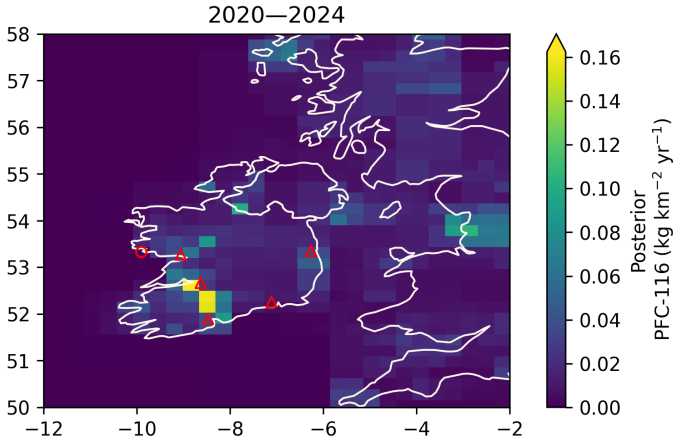

Figure 7.2.2: Spatial distribution of the Irish average modelled emissions of PFC-116 during the period of 2020-2024 (mean from all models). Observing stations are marked with red circles and highly-populated cities are marked with red triangles.

7.3 PFC-218

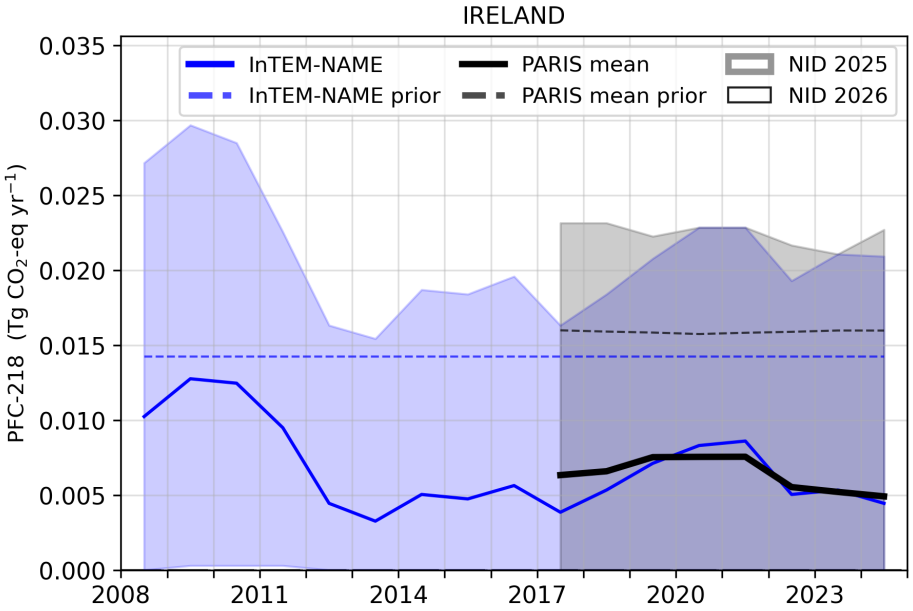

Figure 7.3.1: Verification of the Irish emissions inventory estimates for PFC-218. Modelled annual emissions are given as the mean from all models (black line) and the individual result from InTEM-NAME (blue line). The shaded blue area is the 68 % confidence interval (CI) of InTEM-NAME and the shaded grey area encompasses the 68 % CI from all models. National inventory annual totals from 2025 and 2026 are given as grey and black bars, respectively.

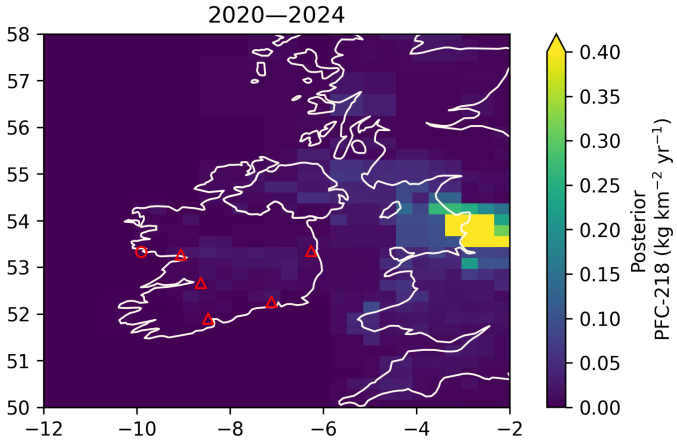

Figure 7.3.2: Spatial distribution of the Irish average modelled emissions of PFC-218 during the period of 2020-2024 (mean from all models). Observing stations are marked with red circles and highly-populated cities are marked with red triangles.

7.4 PFC-318

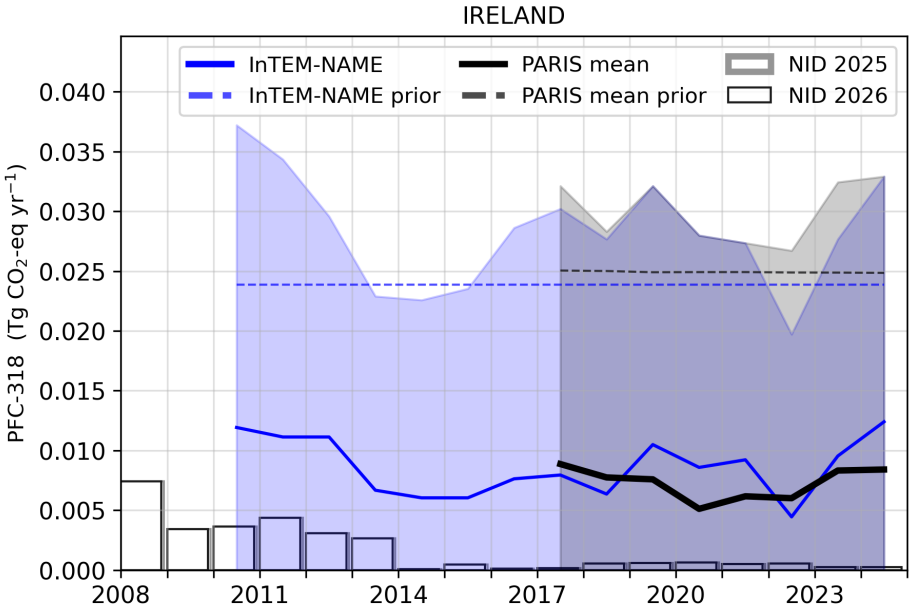

Figure 7.4.1: Verification of the Irish emissions inventory estimates for PFC-318. Modelled annual emissions are given as the mean from all models (black line) and the individual result from InTEM-NAME (blue line). The shaded blue area is the 68 % confidence interval (CI) of InTEM-NAME and the shaded grey area encompasses the 68 % CI from all models. National inventory annual totals from 2025 and 2026 are given as grey and black bars, respectively.

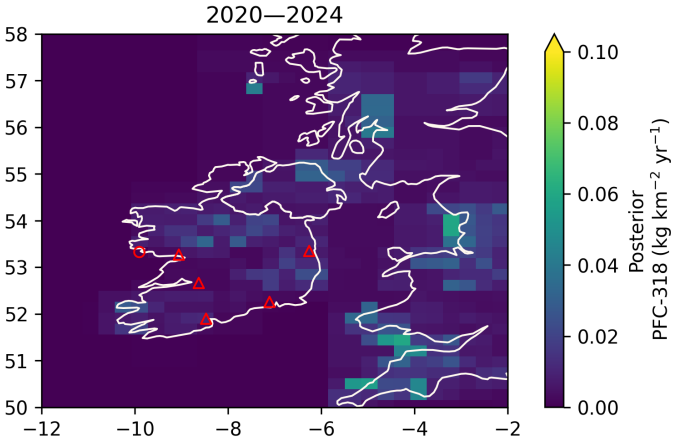

Figure 7.4.2: Spatial distribution of the Irish average modelled emissions of PFC-318 during the period of 2020-2024 (mean from all models). Observing stations are marked with red circles and highly-populated cities are marked with red triangles.

7.5 Total PFCs

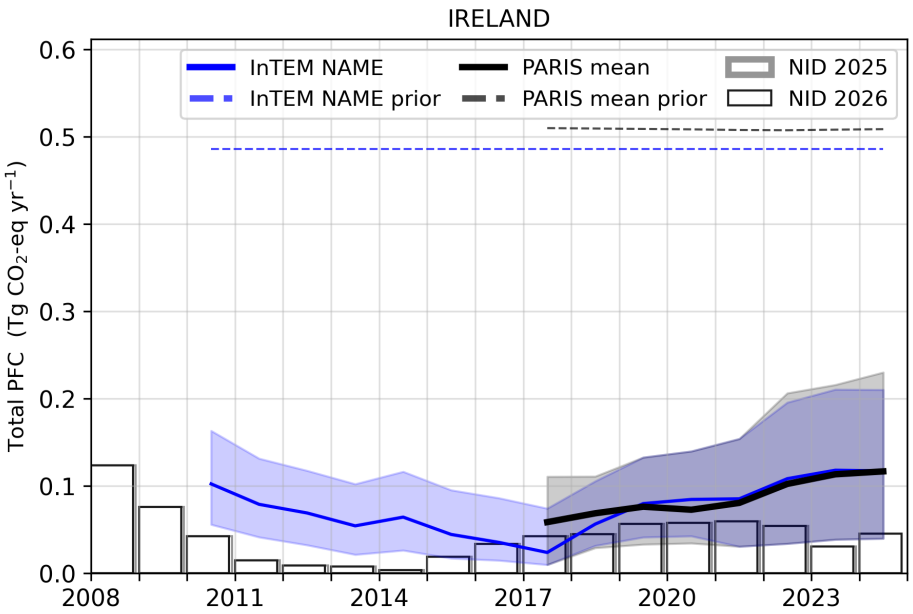

Figure 7.5.1: Verification of the Irish emissions inventory estimates for total PFCs. Modelled annual emissions are given as the mean from all models (black line) and the individual result from InTEM-NAME (blue line). The shaded blue area is the 68 % confidence interval (CI) of InTEM-NAME and the shaded grey area encompasses the 68 % CI from all models. National inventory annual totals from 2025 and 2026 are given as grey and black bars, respectively.

Table 3: Emissions estimation for PFCs according to the National Inventory Document (NID) 2026 and the inversions done in the PARIS project. For the PARIS estimation, the mean of the 3 inversion models is displayed, along with a range of uncertainty estimated via the half distance between the maximum and minimum uncertainties of the different models.

			2020	2021	2022	2023	2024
PFC-14	$GgCO_2\text{-eq} \cdot yr^{-1}$	NID 2026	47	49	40	20	36
		PARIS mean	42 ± 41	44 ± 51	61 ± 73	70 ± 77	77 ± 82
PFC-116	$GgCO_2\text{-eq} \cdot yr^{-1}$	NID 2026	11	9	13	10	9
		PARIS mean	18 ± 21	23 ± 25	30 ± 33	30 ± 31	26 ± 34
PFC-318	$GgCO_2\text{-eq} \cdot yr^{-1}$	NID 2026	0.6	0.5	0.5	0.2	0.2
		PARIS mean	5.1 ± 14.0	6.2 ± 13.7	6.0 ± 13.4	8.3 ± 16.2	8.4 ± 16.5
PFC-218	$GgCO_2\text{-eq} \cdot yr^{-1}$	NID 2026	0.0	0.0	0.0	0.0	0.0
		PARIS mean	7.5 ± 11.4	7.6 ± 11.4	5.5 ± 10.8	5.2 ± 10.5	4.9 ± 11.3

8 Sulphur hexafluoride (SF_6)

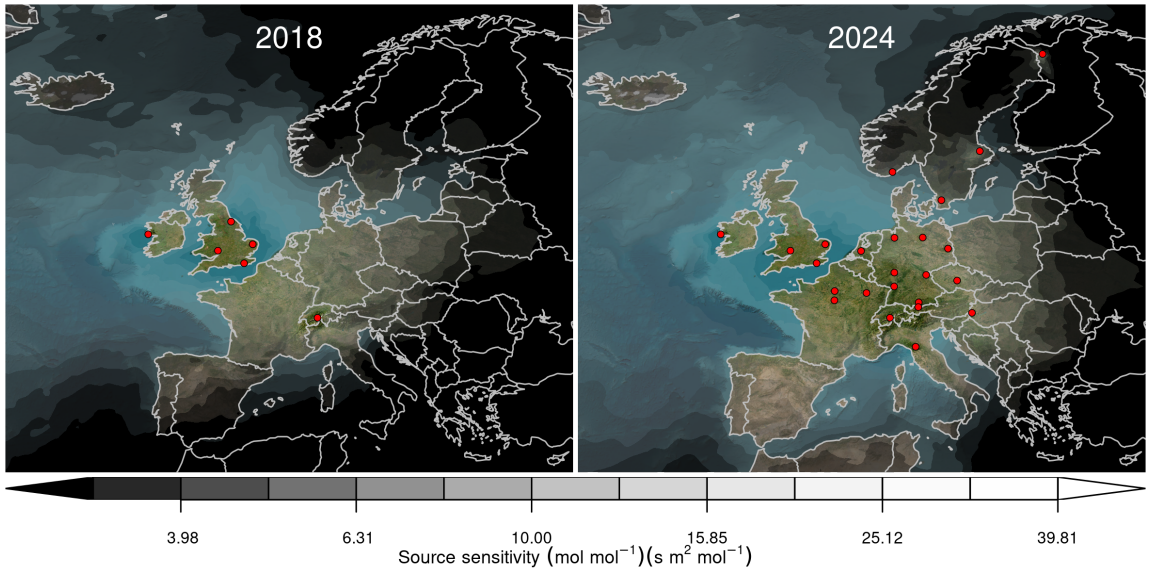

Figure 8.0.1: Total source sensitivity of SF_6 observing sites as calculated by the FLEXPART transport model for the year 2018 (left) and 2024 (right) and used in the inversions. Observing stations active in each year are marked with red dots. Areas with visible land surface represent regions for which emissions can be observed well from the network. Shaded or dark areas represent regions for which limited emission information can be obtained from the network.

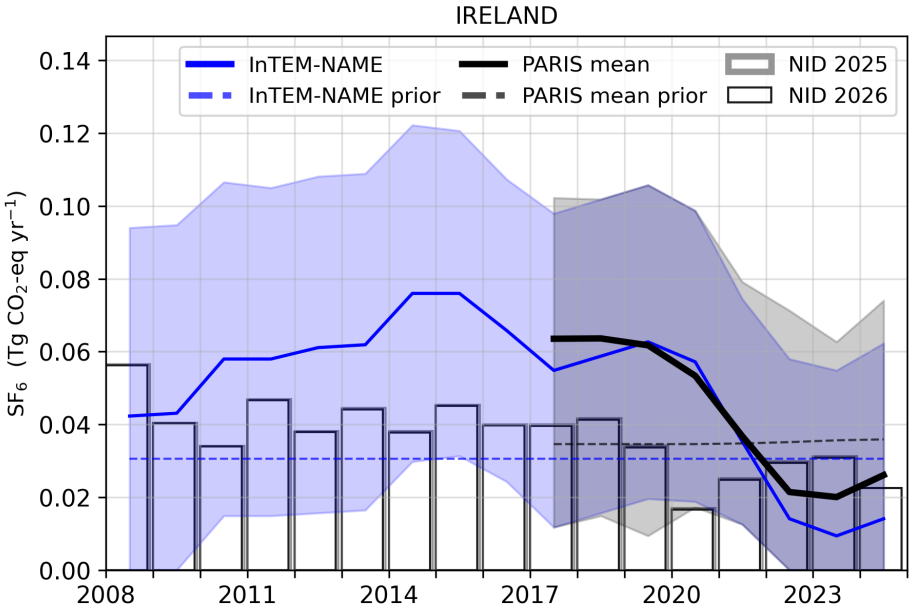

Figure 8.0.2: Verification of the Irish emissions inventory estimates for SF_6. Modelled annual emissions are given as the mean from all InTEM and ELRIS inversions (black line) and the individual result from InTEM-NAME (blue line). The shaded blue area is the 68 % confidence interval (CI) of InTEM-NAME and the shaded grey area encompasses the 68 % CI from all models. National inventory annual totals from 2025 and 2026 are given as grey and black bars, respectively.

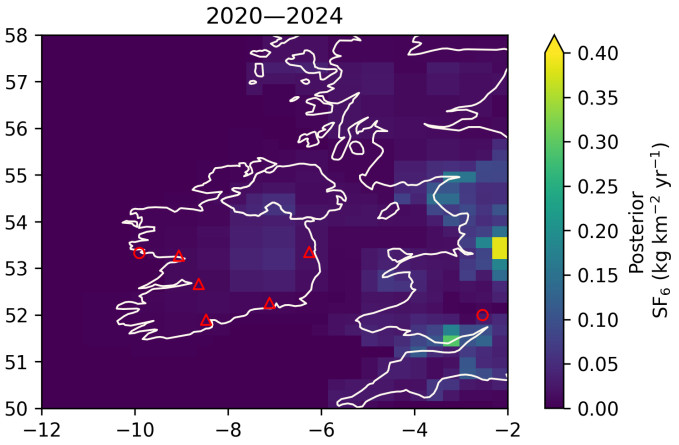

Figure 8.0.3: Spatial distribution of the Irish average modelled emissions of SF_6 during the period of 2020-2024 (mean from all InTEM and ELRIS inversions). Observing stations are marked with red circles and highly-populated cities are marked with red triangles.

9 Nitrogen Trifluoride (NF_3)

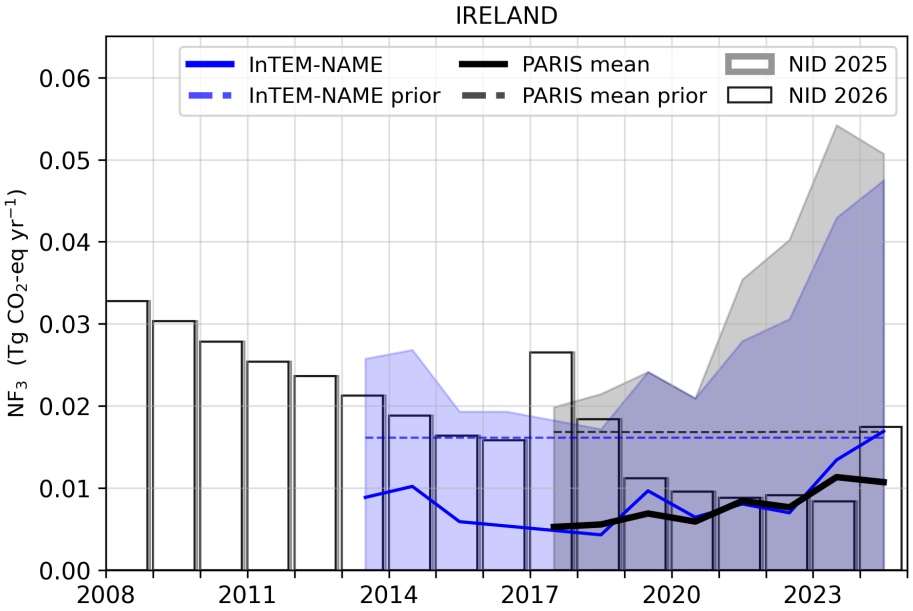

Figure 9.0.1: Verification of the Irish emissions inventory estimates for NF_3. Modelled annual emissions are given as the mean from all models (black line) and the individual result from InTEM-NAME (blue line). The shaded blue area is the 68 % confidence interval (CI) of InTEM-NAME and the shaded grey area encompasses the 68 % CI from all models. National inventory annual totals from 2025 and 2026 are given as grey and black bars, respectively.

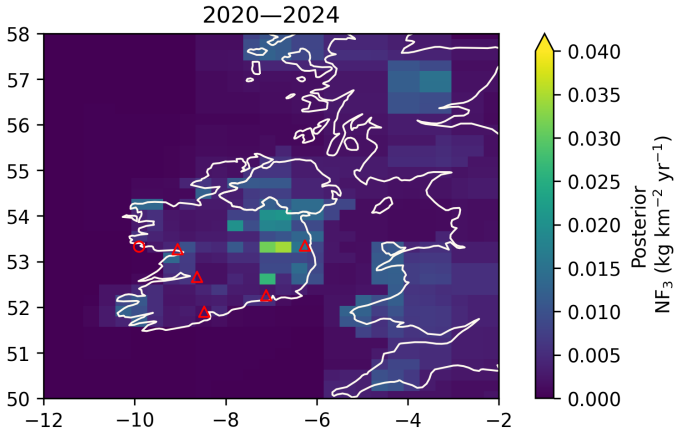

Figure 9.0.2: Spatial distribution of the Irish average modelled emissions of NF_3 during the period of 2020-2024 (mean from all models). Observing stations are marked with red circles and highly-populated cities are marked with red triangles.

10 Carbon Dioxide (CO_2)

Measurements of CO_2 at ICOS sites and related observatories are influenced by a complex combination of sources and sinks. Fossil fuel combustion for transport, heating, energy generation, and other applications produce CO_2, along with other anthropogenic activities such as cement production. The terrestrial and oceanic biosphere produces CO_2 through animal and plant respiration and takes up CO_2 through photosynthesis. Furthermore, CO_2 is exchanged with the ocean through physical and chemical processes.

When considering high-frequency ($\sim$hourly) CO_2 mole fraction deviations from baseline values—used to infer national emissions in regional inverse modelling studies—the influence of biospheric fluxes can be comparable to, or larger than, those of anthropogenic sources (e.g. White et al., 2019). Therefore, research is under way to develop new tracers that can determine fossil fuel CO_2 fluxes independent of biosphere sources and sinks.

Ongoing Horizon Europe projects PARIS and CORSO are examining methods for estimating fossil fuel CO_2 fluxes based on simultaneous measurements of CO_2 and O_2 (Figure 10.0.1). The method relies on the fact that CO_2 and O_2 are inter-converted during combustion and terrestrial biosphere exchange, but with different ratios for the two processes. A quantity can be constructed from these measurements, known as Atmospheric Potential Oxygen (APO), which is insensitive to biosphere fluxes, and may therefore be useful for isolating fossil fuel signals (Pickers et al., 2022).

High-frequency ($\sim$hourly) timeseries of APO are available from Weybourne (WAO, 2010 – present) and Heathfield (HFD, 2021 - present) in the UK (Figure 10.0.1; Pickers, Adcock, and Manning, 2024), and new sites are being established at Cabauw and Zweth in the Netherlands. Preliminary analyses of the WAO data have revealed regional APO trends consistent with the drop in fossil fuel CO_2 emissions during the COVID lockdowns in the UK (Pickers et al., 2022). However, quantification of absolute regional fossil fuel CO_2 emissions remains an area of active research. Recent studies have derived fossil fuel CO_2 emissions for the UK that are highly uncertain (Rigby et al., 2025). Potential confounding factors were identified in Chawner et al. (2024), such as highly uncertain APO fluxes from the ocean, and a poorly constrained regional APO background. These factors are the subject of ongoing research using atmospheric models and new APO measurements from PARIS, CORSO and ICOS.

An alternative method for top-down fossil fuel CO_2 emissions evaluation uses measurements of radiocarbon isotopologues ($^{14}CO_2$, compared to the dominant $^{12}CO_2$). Fossil fuels do not contain ^{14}C, and therefore, their combustion tends to decrease the atmospheric $^{14}CO_2/^{12}CO_2$ ratio. Currently, radiocarbon measurements can only be made at low frequency using flask sampling. However, a relatively intensive flask sampling campaign was carried out across Europe during 2024 as part of CORSO, and the results of this study will be reported on soon.

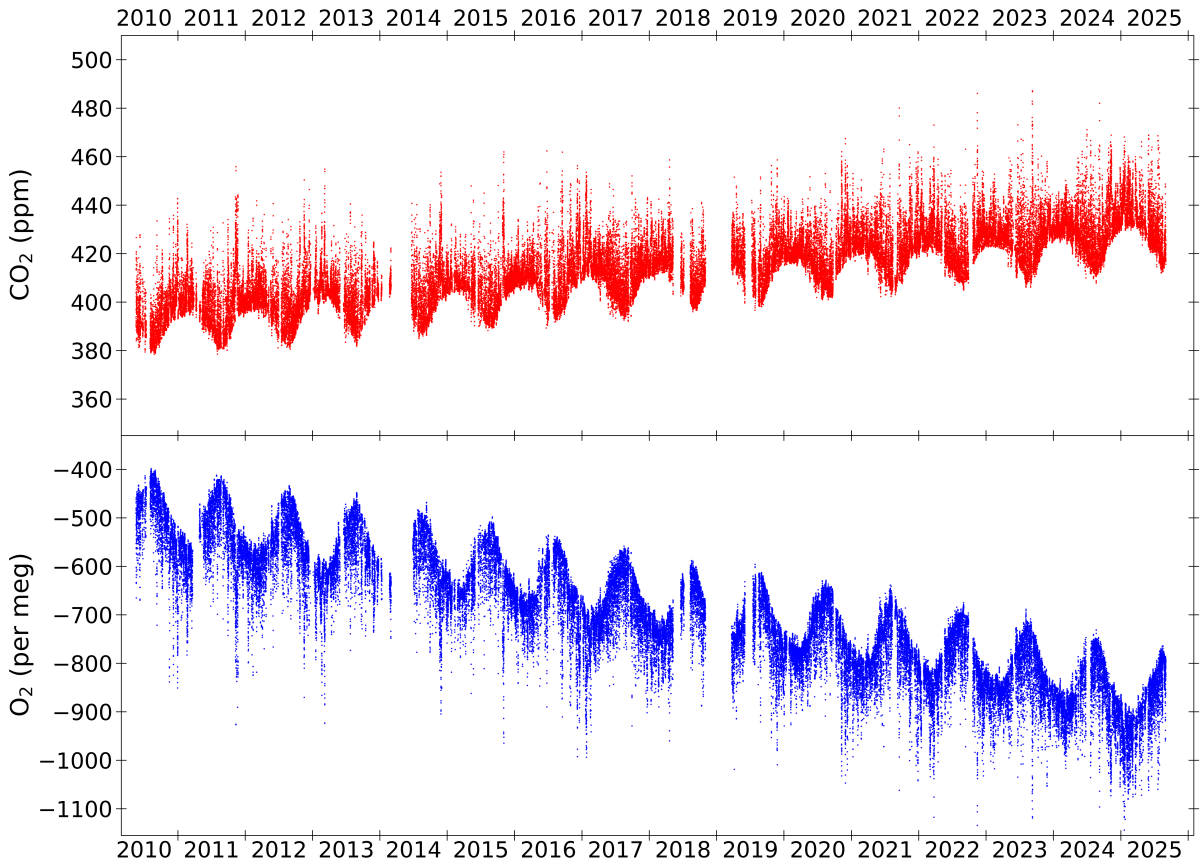

Figure 10.0.1: Carbon dioxide (top, red) and oxygen (bottom, blue) measurements from Weybourne Atmospheric Observatory in the UK, available from the ICOS Carbon Portal (Adcock et al., 2024).

References

Adcock, K. et al. (2024). *Atmospheric GHG data product (o2, o2_stdev, co2, co2_stdev) from Weybourne (10.0 m), 2010-05-19–2023-12-31*. URL: https://hdl.handle.net/11676/j4LzdHQiq3fPgfNeXHruC0Bb.

Chawner, H. et al. (2024). "Atmospheric oxygen as a tracer for fossil fuel carbon dioxide: a sensitivity study in the UK". en. In: *Atmospheric Chemistry and Physics* 24.7, pp. 4231–4252. ISSN: 1680-7324. DOI: 10.5194/acp-24-4231-2024.

European Commission: Joint Research, Centre et al. (2023). *GHG emissions of all world countries – 2023*. Publications Office of the European Union. DOI: 10.2760/953322.

Ganesan, A. L. et al. (2014). "Characterization of uncertainties in atmospheric trace gas inversions using hierarchical Bayesian methods". In: *Atmospheric Chemistry and Physics* 14.8, pp. 3855–3864. DOI: 10.5194/acp-14-3855-2014.

Ganesan, A. L. et al. (2015). "Quantifying methane and nitrous oxide emissions from the UK and Ireland using a national-scale monitoring network". In: *Atmos. Chem. Phys.* 15.11, pp. 6393–6406. DOI: 10.5194/acp-15-6393-2015.

Henne, S. et al. (2016). "Validation of the Swiss methane emission inventory by atmospheric observations and inverse modelling". In: *Atmospheric Chemistry and Physics* 16.6, pp. 3683–3710. DOI: 10.5194/acp-16-3683-2016.

Jones, A.R. et al. (2007). "The U.K. Met Office's next-generation atmospheric dispersion model, NAME III, in Borrego C. and Norman A.-L. (Eds)". In: *Air Pollution Modeling and its Application XVII (Proceedings of the 27th NATO/CCMS International Technical Meeting on Air Pollution Modelling and its Application), Springer*, pp. 580–589. DOI: 10.1007/978-0-387-68854-1_62.

Katharopoulos, I. et al. (2023). "Impact of transport model resolution and a priori assumptions on inverse modeling of Swiss F-gas emissions". In: *Atmos. Chem. Phys.* 23.22, pp. 14159–14186. DOI: 10.5194/acp-23-14159-2023.

Manning, A. J. et al. (2021). "Evidence of a recent decline in UK emissions of hydrofluorocarbons determined by the InTEM inverse model and atmospheric measurements". In: *Atmospheric Chemistry and Physics* 21.16, pp. 12739–12755. DOI: 10.5194/acp-21-12739-2021.

Pickers, P., K. Adcock, and A. Manning (2024). *Atmospheric oxygen and carbon dioxide observations from Weybourne Atmospheric Observatory, Norfolk, UK uploaded to public archives*. Tech. rep. Process Attribution of Regional Emissions (PARIS). URL: https://horizoneurope-paris.eu/wp-content/uploads/sites/914/2024/07/PARIS-deliverables-D6.1-High-frequency-APO-data-uploaded-final.pdf.

Pickers, P. A. et al. (2022). "Novel quantification of regional fossil fuel CO2 reductions during COVID-19 lockdowns using atmospheric oxygen measurements". en. In: *Science Advances* 8.16, eabl9250. ISSN: 2375-2548. DOI: 10.1126/sciadv.abl9250.

Rigby, M. et al. (2019). "Increase in CFC-11 emissions from eastern China based on atmospheric observations". In: *Nature* 569, pp. 546–550. DOI: 10.1038/s41586-019-1193-4.

Rigby, M. et al. (2025). *Inverse estimates of fossil fuel CO2 emission*. Tech. rep. Process Attribution of Regional Emissions (PARIS). URL: https://horizoneurope-paris.eu/wp-content/uploads/sites/914/2025/01/PARIS-M24-Inverse-estimates-of-fossil-fuel-CO2-emissions-final.pdf.

Stohl, A. et al. (2005). "Technical note: The Lagrangian particle dispersion model FLEXPART version 6.2". In: *Atmospheric Chemistry and Physics* 5, pp. 2461–2474. DOI: 10.5194/acp-5-2461-2005.

White, E. D. et al. (2019). "Quantifying the UK's carbon dioxide flux: an atmospheric inverse modelling approach using a regional measurement network". en. In: *Atmospheric Chemistry and Physics* 19.7, pp. 4345–4365. ISSN: 1680-7324. DOI: 10.5194/acp-19-4345-2019.